CENTENNIAL FEATURE ARTICLE

Quantum Dot Solar Cells. Semiconductor Nanocrystals as Light Harvesters†

Prashant V. Kamat*

Notre Dame Radiation Laboratory Department of Chemistry & Biochemistry and Department of Chemical & Biomolecular Engineering, Notre Dame, Indiana 46556

Received: July 30, 2008; Revised Manuscript Received: August 26, 2008

The emergence of semiconductor nanocrystals as the building blocks of nanotechnology has opened up new ways to utilize them in next generation solar cells. This paper focuses on the recent developments in the utilization of semiconductor quantum dots for light energy conversion. Three major ways to utilize semiconductor dots in solar cell include (i) metal−semiconductor or Schottky junction photovoltaic cell (ii) polymer−semiconductor hybrid solar cell, and (iii) quantum dot sensitized solar cell. Modulation of band energies through size control offers new ways to control photoresponse and photoconversion efficiency of the solar cell. Various strategies to maximize photoinduced charge separation and electron transfer processes for improving the overall efficiency of light energy conversion are discussed. Capture and transport of charge carriers within the semiconductor nanocrystal network to achieve efficient charge separation at the electrode surface remains a major challenge. Directing the future research efforts toward utilization of tailored nanostructures will be an important challenge for the development of next generation solar cells.

A. Nanoscience Opportunities

New initiatives to harvest incident photons with greater efficiency are needed to meet our demand of clean energy.[1−4] The single crystal silicon based photovoltaic devices that are commercially available for installation deliver power with a ∼15% efficiency. These *first generation* devices suffer from high cost of manufacturing and installation. The *second generation* devices consisting of polycrystalline semiconductor thin films can bring down the price significantly, but their efficiency needs to be enhanced for making them practically viable. Now the focus is on the *third generation* devices that can deliver high efficiency devices at economically viable cost.

In recent years nanomaterials have emerged as the new building blocks to construct light energy harvesting assemblies. Efforts are being made to design organic and inorganic hybrid structures that exhibit improved selectivity and efficiency toward light energy conversion. Of particular interest are the size dependent properties such as size quantization effects in semiconductor nanoparticles and quantized charging effects in metal nanoparticles.[5−11] Recent efforts to synthesize nanostructures with well defined geometrical shapes (e.g., solid and hollow spheres, prisms, rods, tubes, and wires) and organize them as 2- and 3-dimensional assemblies have further expanded the possibility of developing new strategies for light energy conversion.[12−30]

Quantum dot based solar cells have drawn a lot of attention during past few years because of the possibility of boosting the energy conversion efficiency beyond the traditional Shockley and Queisser limit of 32% for Si based solar cells.[31] Three different types of solar cells that capitalize salient properties of semiconductor nanocrystals have emerged: (i) metal−semiconductor or Schottky junction photovoltaic cell, (ii) semiconductor nanostructure-polymer solar cell, and (iii) semiconductor sensitized quantum dot solar cell (Figure 1).

Specific advantages to using semiconductor quantum dots as light harvesting assemblies in solar cells exist.[32] First and foremost, their size quantization property allows one to tune the visible response and vary the band offsets to modulate the vectorial charge transfer across different sized particles.[33] In addition, these quantum dots open up new ways to utilize hot electrons[34] or generate multiple charge carriers with a single photon.[35,36] Multiple carrier generation in PbSe nanocrystals has shown that two or more excitons can be generated with a single photon of energy greater than the bandgap.[35,37,38] These recent developments of photoinduced charge separation semiconductor nanocrystal based assemblies and efforts to utilize them in solar cells are reviewed here.

B. Charge Separation in Semiconductor Composites. Early Studies

Photoinduced charge separation in semiconductor nanoparticles has been studied since the early 1980s.[5,11,39,40] Although the charge recombination dominates in a nanometer sized semiconductor particle, the charge separation can be greatly improved by coupling it with another semiconductor particle having favorable energetics. In addition, semiconductors such as CdS,[41−43] PbS,[44,45] Bi_2S_3,[44,46,47] CdSe,[48−50] and InP,[51] which absorb light in the visible, can serve as sensitizers as they are

† This year marks the Centennial of the American Chemical Society's Division of Physical Chemistry. To celebrate and to highlight the field of physical chemistry from both historical and future perspectives, *The Journal of Physical Chemistry* is publishing a special series of Centennial Feature Articles. These articles are invited contributions from current and former officers and members of the Physical Chemistry Division Executive Committee and from *J. Phys. Chem.* Senior Editors.

* To whom correspondence should be addressed. E-mail: pkamat@nd.edu. Web: http://www.nd.edu/∼pkamat.

10.1021/jp806791s CCC: $40.75
Published on Web 10/18/2008

Prashant V. Kamat is currently a Professor of Chemistry and Biochemistry, a Senior Scientist at Radiation Laboratory, and a Concurrent Professor in the Department of Chemical and Biomolecular Engineering, University of Notre Dame. A native of Binaga, India, he earned masters (1974) and doctoral degrees (1979) in Physical Chemistry from the Bombay University, and carried out his postdoctoral research at Boston University (1979−1981) and University of Texas at Austin (1981−1983). He joined Notre Dame Radiation Laboratory in 1983 and initiated the photoelectrochemical investigation of semiconductor nanoparticles. Dr. Kamat's research has made significant contributions to three areas: (1) photoinduced catalytic reactions using semiconductor and metal nanoparticles, nanostructures, and nanocomposites, (2) developing inorganic−organic hybrid assemblies for utilizing renewable energy resources, and (3) environmental remediation using advanced oxidation processes and chemical sensors. He has directed DOE funded solar photochemistry research for more than 20 years. He has published more than 350 peer-reviewed journal papers, review articles, and book chapters. He has edited two books in the area of nanoscale materials. He was a fellow of Japan Society for Promotion of Science during 1997 and 2003 and was presented the 2006 Honda-Fujishima Lectureship award by the Japan Photochemical Society. In 2008 he was elected a Fellow of the Electrochemical Society.

able to transfer electrons to large bandgap semiconductors such as TiO_2 or SnO_2 (Figure 2). Improved charge separation and enhanced photocatalytic efficiency of such composite nanostructures have been extensively studied by our group[52−57] and other research groups.[43,58−64] Readers may refer to earlier reviews to obtain charge transfer and charge rectification in various semiconductor composite systems.[65−68]

By controlling the particle size of quantum dots one can vary the energetics of the particles. Increased band energies of Q-dots can thus be utilized to promote,[44] suppress,[57] or rectify[48,69] the electron transfer between two semiconductor nanostructures. Such composite structures rectify the flow of charge carriers and improve the photocatalytic performance or photoelectrochemical performance of nanostructure semiconductor based systems. For example, nearly ten times enhancement in the photocatalytic efficiency has been achieved by coupling TiO_2 and SnO_2 systems.[53,55] Similarly, composites of ZnO-CdS,[70] TiO_2−SnO_2,[71] SnO_2−CdSe,[72] and SnO_2−CdS[56] have been successfully used to promote efficient charge separation and charge propagation in dye-sensitized solar cells.

Most of the early studies on semiconductor nanocrystals reported to-date have been limited to elucidation of photophysical and photochemical properties[5,73−77] or their use as biological probes.[78−83] One of the early studies on the TiO_2−CdSe system highlighted the possibility of rectification behavior of the composite system and its usefulness in improving the overall performance of nanostructured semiconductor systems.[48,69] Transient absorption studies indicated intense bleaching of the excitonic band as the CdS[84−86] and CdSe[87] particles were subjected to bandgap excitation. Such bleaching that directly represents charge separation in semiconductor nanocrystal was explained on the basis of band filling model[86,88] as well as Stark effect.[89−91] The electrons trapped within TiO_2 nanoparticles following the laser excitation of CdS-TiO_2 system were characterized by femtosecond transient absorption spectroscopy.[92]

C. Charge Separation in Semiconductor Nanocrystals. Recent Advances

Semiconductor nanocrystals when subjected to bandgap excitation undergo charge separation (Reactions 1 and 2 represent charge separation and recombination of CdSe nanocrystals respectively. Subscripts s and p refer to the electronic states of the electrons (e) and holes (h)).

$$\mathrm{CdSe} + h\nu \rightarrow \mathrm{CdSe}\ (e_p + h_p) \rightarrow \mathrm{CdSe}\ (e_s + h_s) \quad (1)$$

$$\mathrm{CdSe}\ (e_s + h_s) \rightarrow \mathrm{CdSe} + h\nu' \quad (2)$$

As the electrons and holes accumulate in the conduction and valence bands, one observes bleaching in the absorption. The charge separated state can be followed by the emission decay or the recovery of the transient bleaching.[74,75,93−102] Figure 3 compares the emission yield and decay of CdSe quantum dots anchored on glass slides and TiO_2 films. The significant quenching seen in these emission measurements confirms the electron transfer between excited CdSe and TiO_2 as the major deactivation pathway for the observed quenching of emission.

$$\mathrm{CdSe}\ (e_s + h_s) + TiO_2 \rightarrow \mathrm{CdSe}\ (h) + TiO_2(e) \quad (3)$$

The deactivation of the excited semiconductor nanocrystals can be modulated by applying electrochemical bias.[103] Mulvaney and co-workers[104] have demonstrated that the photobrightening and charge carrier injection are coupled processes. The photoluminescence (PL) of CdSe/CdS/ZnS semiconductor nanocrystals deposited on gold substrates is reversibly quenched at negative potentials in nitrogen atmosphere. However, when a negative potential is applied to the semiconductor nanocrystalline film in aerated acetonitrile, the PL intensity increased.

Figure 4, panels A and B, shows the ground-state absorption spectra and transient absorption spectra of different size CdSe quantum dots in the visible region recorded 2 ps after 387 nm laser pulse (pulse width 130 fs) excitation. The ultraband excitation initially excites electrons to the higher p-state which then quickly relaxes to low lying s-state. The bleaching at the band edge seen in the transient absorption in Figure 4B provides a means to probe the fate of electrons accumulated in the thermally relaxed s-state. Sargent and co-workers have found dominance of Auger recombination rate in PbS quantum dots if more than one fundamental exciton is excited per dot.[105] Based on the saturation in the bleaching signal they concluded that additional excitons do not contribute to absorption saturation, in contrast to CdSe.[105] The shape of the semiconductor nanocrystal also affects the excited-state dynamics. For example, CdSe nanorod samples with the same length (∼30 nm) but with different diameters, 2.5 and 8.0 nm, exhibit 8 times faster intraband energy relaxation for thicker rods than thin rods.[106] The multiple charge carrier generation in semiconductor nanocrystals has also drawn much interest for its possible implementation in solar cells. The details on the photogeneration and recombination of multiexcitons in semiconductor nanocrystals and their implication in solar cells have been reviewed recently by Klimov.[100]

When in contact with another semiconductor, the excited CdSe quantum dots are capable of injecting electrons into TiO_2 nanoparticles.[49,108] The TiO_2 particle has a band gap of 3.2 eV, exhibiting absorption in the UV region with onset around 390

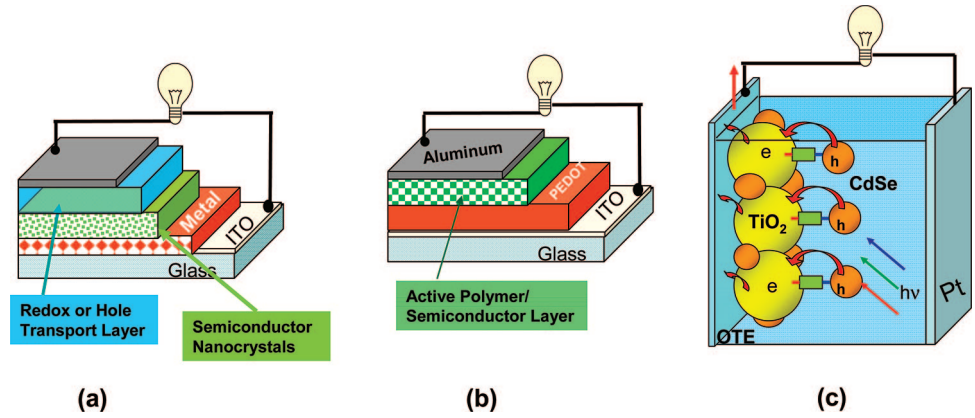

Figure 1. Schematic diagram showing the strategies to develop quantum dot (semiconductor nanocrystal) based solar cells: (a) metal−semiconductor junction, (b) polymer−semiconductor, and (c) semiconductor−semiconductor systems.

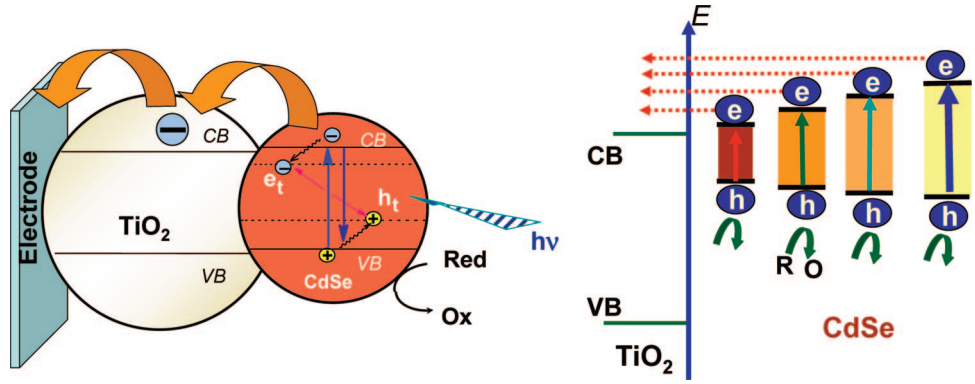

Figure 2. Charge injection of excited CdSe quantum dot into TiO_2 nanoparticle. The scheme on the right shows the modulation of energy levels (and hence the charge injection) by size control.

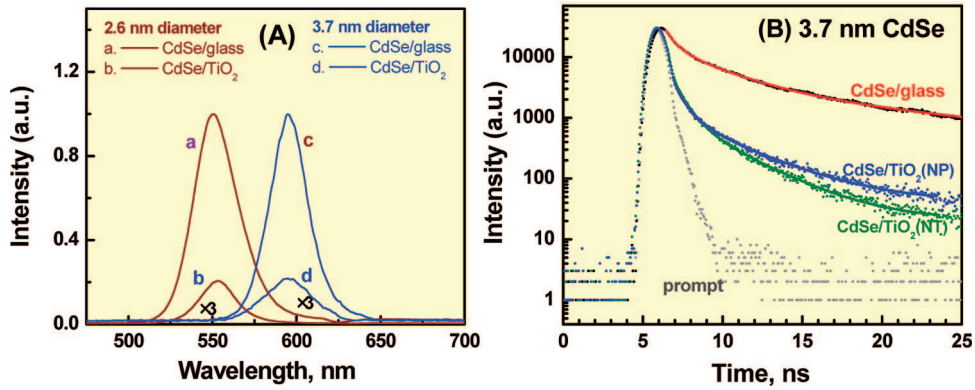

Figure 3. (A) Emission spectra of 2.6 and 3.7 nm diameter CdSe quantum dot film deposited on glass and OTE/TiO_2 (nanoparticle) films. (B) Emission lifetimes of 3.7 nm CdSe quantum dots deposited on glass, TiO_2 nanoparticle film and TiO_2 nanotubes (monitoring wavelength 580 nm). (From ref 33.)

nm. By employing mercaptopropionic acid (MPA) as a linker molecule, it is possible to bring together TiO_2 and CdSe nanoparticles. For 7.5 nm diameter CdSe colloids the conduction band is estimated to be −0.8 V vs NHE[103] and it shifts to negative potentials with decreasing particle size (e.g., −1.57 V vs NHE for 3.0 nm particles). Because of the small electron effective mass $m_e = 0.13m_o$ versus the significantly larger hole mass $m_h = 1.14m_o$, most of the band gap increase is seen as a shift in the conduction band to more negative potentials (vs NHE).[93] Thus, CdSe quantum dots with their increased band gaps are expected to have favorable conduction band energies for injecting electrons into TiO_2 (reaction 3).

The effect of the TiO_2 interaction with excited CdSe quantum dots can be seen from the bleaching recoveries recorded in Figure 4, panels C and D. The additional deactivation pathway of electron transfer to TiO_2 causes a faster recovery of the bleaching (Figure 4D). With decreasing particle size the bleaching recovery occurs at a faster rate. The rate constant can be estimated by comparing the bleaching recovery lifetimes in the presence and absence of TiO_2 (expression 4).

$$k_{et} = 1/\tau_{(CdSe+TiO_2)} - 1/\tau_{CdSe} \quad (4)$$

Electron transfer kinetics can be evaluated in terms of Marcus theory[109,110] for a nonadiabatic reaction in the classical activation limit. The theory implies that the logarithm of the electron transfer rate is a quadratic function with respect to the driving force, $-\Delta G$. This expression has been successfully applied by Hupp[111] and others[112,113] to investigate charge recombination kinetics in dye-sensitized SnO_2 and TiO_2 systems. As the driving force, $-\Delta G$, (viz., energy difference between the acceptor and

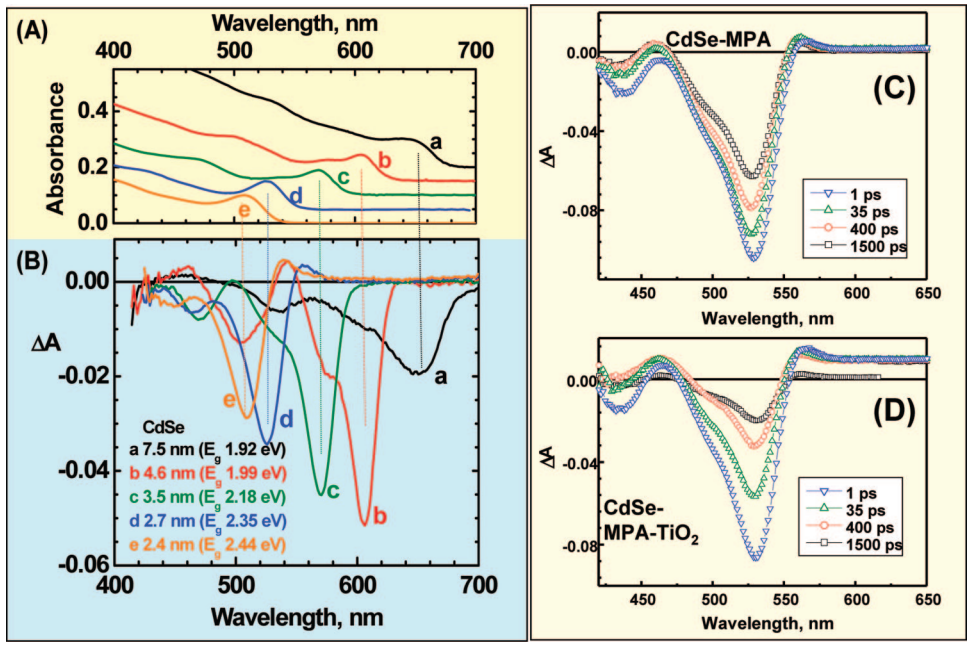

Figure 4. (A) Absorbance spectra of CdSe quantum dots in toluene. (*Y*-axis offset is introduced for clarity.) (B) Transient absorption spectra recorded 2 ps following the 387 nm laser pulse excitation of different size CdSe quantum dots in 1:1 ethanol:tetrahydrofuran (THF). Time resolved spectra recorded following laser pulse excitation of 3 nm CdSe quantum dots in the (C) absence and (D) presence of TiO_2 are also shown. (From refs 107 and 49.)

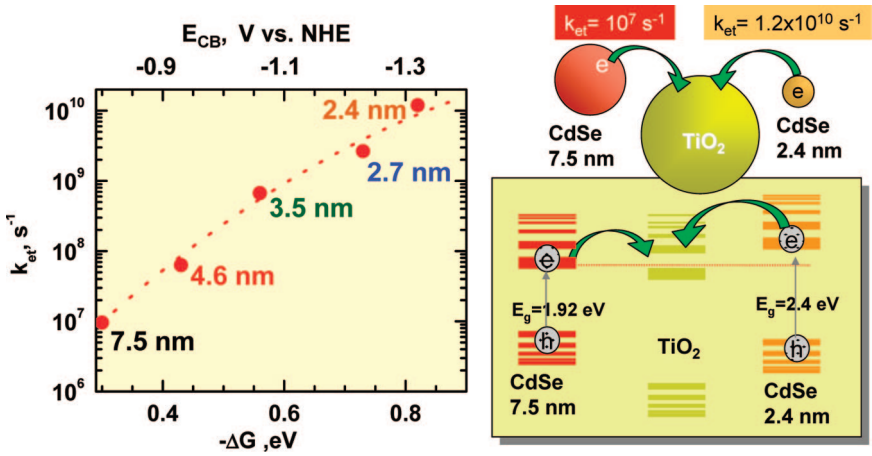

Figure 5. Left: The dependence of electron transfer rate constant on the energy difference between the conduction bands. Right: Scheme illustrating the principle of electron transfer from two different size CdSe quantum dots into TiO_2 nanoparticle. (From ref 107.)

donor systems) increases, the rate of ET increases, reaching a maximum when the driving force equals the reorganization energy (i.e., when the activation free energy $\Delta G^* = 0$). Similar observation has also been confirmed recently by Lian and co-workers during the investigation of CdSe QDs adsorbed with $Re(CO)_3Cl(dcbpy)$ (dcbpy) 4,4′-dicarboxy-2,2′-bipyridine).[114]

The driving force for the electron transfer between CdSe and TiO_2 is dictated by the energy difference between the conduction band energies. The conduction band of TiO_2 is at −0.5 V versus NHE.[115] If we assume the larger CdSe particles have band energy close to the reported value of −0.8 V vs NHE,[103] we can use the increase in bandgap as the increase in driving force ($-\Delta G$) for the electron transfer. Since the shift in the conduction band energy is significantly greater than the shift in valence band energy for quantized particles,[93] we can expect the conduction band of CdSe QDs to become more negative (on NHE scale) with decreasing particle size. Figure 5 shows the energy gap dependence of $\log(k_{et})$. As the particle size decreases, we see an enhanced electron transfer rate. The driving force of 0.8 eV is at or close to the reorganization energy and hence we expect a normal Marcus region in which the rate of electron transfer increases with the driving force. This small energy difference attained by decreasing particle size is sufficient to increase the electron transfer rate by nearly 3 orders of magnitude.

The fastest electron transfer in the CdSe−TiO_2 system was observed with 2.4 nm-CdSe quantum dots. The rate constant of $\sim 1.2 \times 10^{10}$ s^{-1} in this experiment reflects an average lifetime of 83 ps. Other femtosecond transient studies have reported similar electron transfer rates between excited CdS/CdSe QDs and TiO_2 on a time scale of 2−50 ps.[116,117] Size-dependent electronic properties of semiconductor QDs are regarded as one of the most attractive features for attaining a band gap gradient in quantum dot solar cells. The dependence of the charge injection rate constant on particle size demonstrates the possibility of modulating the electron transfer rate between CdSe and TiO_2 particles by making use of size quantization effects.

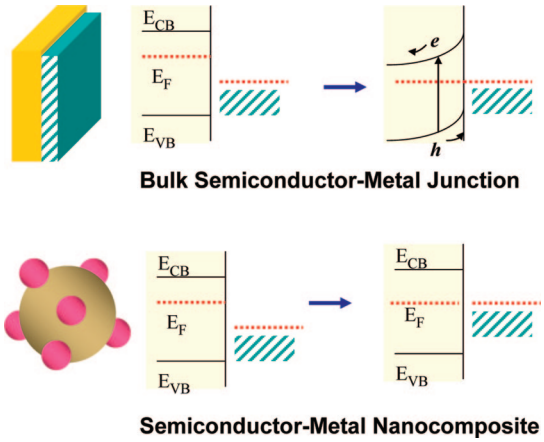

Figure 6. Fermi level equilibration at bulk metal-nanocrystal (top) and metal nanoparticle-semiconductor nanoparticle junction (bottom).

D. Toward the Development of Next Generation Solar Cells

a. Semiconductor−Metal (or Schottky) Junction Solar Cell. When a semiconductor comes in contact with a metal surface it undergoes Fermi level equilibration. For a bulk semiconductor (e.g., single crystal) the conduction and valence bands bend to form a space charge region. The space charge layer, which is dependent on the carrier density, can extend up to a few microns. When such semiconductor-metal junction is subjected to bandgap excitation (e.g., in photovoltaic cell), the band bending rectifies the flow of photogenerated charge carriers to produce photocurrent in a solar cell. In the case of semiconductor nanocrystals, the electrons are confined and the individual nanocrystal remains isoenergetic. As a result of this size limitation the bands remain flat and the charge separation is essentially dictated by the Fermi level equilibration (Figure 6). Different degrees of electron accumulation can make the nanocrystal attain different Fermi levels and thus create an energy gradient to drive the electrons toward the collecting electrode.[118−120]

The Fermi level (E_F) of the semiconductor is directly related to the number of accumulated electrons as illustrated in expression 5.

$$E_F = E_{CB} + kT \ln n_c/N_c \quad (5)$$

E_{CB} is the conduction band energy level versus NHE, n_c is the density of accumulated electrons, and N_c is the charge carrier density of the semiconductor.

If the metal in contact with the semiconductor quantum dot is also in the particulate form we can expect electron storage within the particles. For example, Au nanoparticles possess the property of storing electrons in a quantized fashion.[121,122] The double-layer charging around the metal nanoparticle facilitates storage of the electrons within the gold nanoparticle. When the semiconductor and metal nanoparticles are in contact, the photogenerated electrons are distributed between the semiconductor and metal nanoparticles.[123−126] Since the electron accumulation increases the Fermi level of the metal to more negative potentials, the resultant Fermi level of the composite shifts closer to the conduction band of the semiconductor.

For example, if one accumulates more electrons in the TiO_2 or TiO_2/Au system a negative shift in the Fermi level of the TiO_2 is expected to occur. By shifting the Fermi level closer to the conduction band it would therefore be possible to improve the energetics of the semiconductor particle systems.

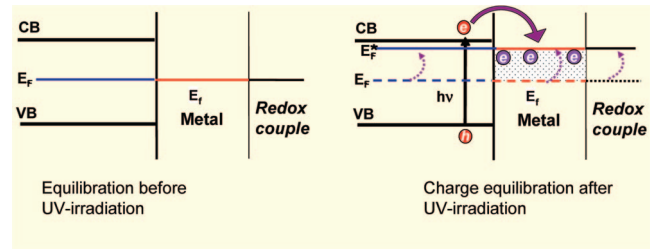

Figure 7. Equilibration of semiconductor-metal nanocomposites with the redox couple before and after UV−irradiation. Electron storage in metal nanostructure causes Fermi level to shift closer to conduction band of the semiconductor. (From ref 127.)

The apparent Fermi levels of the TiO_2 and TiO_2/Au nanoparticle systems can be determined by attaining a Nernstian equilibrium with a known redox couple (viz., C_{60}/C_{60}^-).[127] The apparent Fermi level (E_F*) was correlated to the concentration of the redox species by using expression 6.[126,128,129]

$$E_F^*(TiO_2(e)) = E_{fb} = E^\circ_{Ox/Red} + 0.059 \log([Ox]_{eq}/[Red]_{eq}) \quad (6)$$

where E_F* and E_{fb} are the apparent Fermi level and the flat band potential of TiO_2 (or TiO_2/Au), respectively, and $E^\circ_{Ox/Red}$ is the standard reduction potential of the redox couple (viz., $E^\circ(C_{60}/C_{60}^{\bullet-})$ −0.25 V versus NHE). By determining the equilibrium concentration of C_{60}^- in the UV-irradiated TiO_2 and TiO_2/Au suspension from the absorption at 1075 nm (ε = 16 000 M^{-1} cm^{-1}), we can obtain the values of E_F* (expression 6). In the absence of a noble metal, the apparent Fermi level of TiO_2 is around −230 mV versus NHE for TiO_2 particulate system. As the TiO_2 particles come in contact with Au nanoparticles, the apparent Fermi level shifts to negative potentials.

A similar shift in the Fermi level of the composite system was also observed for the ZnO−Au systems.[124,125] The negative shift in the Fermi level is an indication of improved charge separation and more reductive power for the composite system. Figure 7 illustrates the shift in the Fermi level of the composite as a result of charge equilibration between semiconductor and metal nanoparticles.

The particle size of the metal also influences the shift in apparent Fermi level. The apparent Fermi levels for TiO_2/Au system were determined to be −250, −270, and −290 mV vs. NHE for 8, 5, and 3 nm size gold nanoparticles respectively. Since the energy levels in the gold nanoparticles are discrete, one expects a greater shift in the energy level for each accumulated electron in smaller size Au nanoparticles than in larger ones. Thus, the composite with smaller Au nanoparticles is expected to be more reductive than the one with larger Au nanoparticles. These observations parallel the size-dependent catalytic properties of gold nanoparticles deposited on titania in earlier studies.[130]

Efforts have been made to self-assemble gold nanoparticles and CdS or CdSe quantum dots using thiol linkers and characterize their photophysical and charge transfer properties.[131−133] Charge injection and charge transport in thin disordered films of CdSe nanocrystals between metal electrodes have been probed by monitoring current−voltage characteristics of photovoltaic devices.[134] The rectifying behavior of such a device pointed out that high work function materials such as gold and indium−tin oxide are poor electron injectors in agreement with the estimated conduction and valence band levels of the nanocrystals. Willner and co-workers,[135−137] who studied the

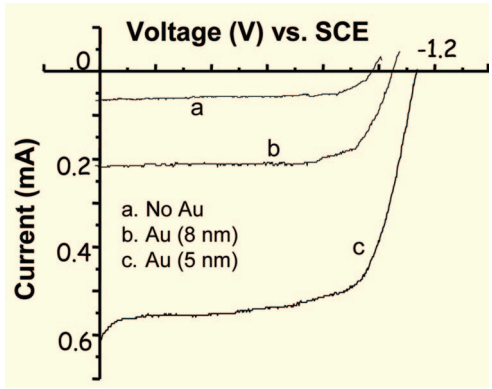

Figure 8. *I*−*V* characteristics of (a) TiO_2, (b) TiO_2/Au (8-nm diameter), and (c) TiO_2/Au (5-nm diameter) composite film. Measurements were performed in a three-arm cell with Pt as counter electrode, a saturated calomel electrode as reference, and 3 mL of 0.05 M NaOH as electrolyte. UV light from xenon lamp ($\lambda > 300$ nm) was used as the excitation source. (From reference 125.)

photoelectrochemical performance of self-assembled CdS nanocrystals on gold surfaces have observed that redox properties of bridging unit such as dianiline play an important role in transporting the electrons from the semiconductor nanoparticles to the electrode. A recent study highlights hybrid gold-tipped CdSe nanorods (nanodumbbells) for visible light photocatalysis.[138] Under visible light irradiation, charge separation takes place between the semiconductor and metal parts of the hybrid particles which in turn induces photocatalytic reduction. Excited state deactivation processes of CdS or CdSe particles can provide further insight into energy[139,140] and electron transfer[141,142] pathways between the excited semiconductor and metal nanocomposites.

The beneficial effect of Fermi level equilibration between semiconductor-metal nanoparticles can be seen from the photoelectrochemical behavior of nanostructured semiconductor films.[125,126,143] Figure 8 shows the current−voltage characteristics of TiO_2 and TiO_2/Au films cast on conducting glass electrodes, which were recorded in a photoelectrochemical cell using 0.05 M NaOH solution as the electrolyte.

The zero-current potential, which corresponds to apparent flat band potential of the nanostructured semiconductor film, shifts to negative potentials with the deposition of Au nanoparticles. The shifted apparent flat band potentials are observed at −1.04 and −1.14 V versus SCE for electrodes modified with 8 and 5 nm gold nanoparticles respectively. The observed photocurrents at positive bias are significantly higher for the composite films involving Au nanoparticles. These photoelectrochemical measurements further confirm the effect of noble metals in improving the energetics of the semiconductor nanostructures.

Although Schottky junction based quantum dot solar cells are yet to be exploited fully, their importance is being realized in recent findings. For example, Sargent and co-workers have reported solution-processed infrared responsive photovoltaic devices based on PbS quantum dots.[105,144−146] One such example involves spin casting of thin films of PbS quantum dots (total thickness of 210−250 nm) on ITO (indium tin oxide) substrates and then treating with a surface modifier (e.g., benzenedithiol treatment). A metal contact layer consisting of 100 nm Mg/190 nm Ag was then made by thermal evaporation through a shadow mask.[147] Using a contact area of 3.1 mm^2 a power conversion efficiency of 3.6% in the infrared and 1.1% under simulated solar illumination at 100 mW/cm^2 was reported.[147] Further advances in this area could lead to the development of low-cost, large-area, physically flexible solar cells.

b. Organic Solar Cell. The solution processibility and attractive photoconversion efficiency have focused significant attention on organic semiconductor materials for constructing solar cells.[149] The heterojunctions of regioregular polymers (e.g., poly(3-hexylthiophene or P3HT) and a soluble fullerene derivative (for example, [6,6]-phenyl C-61-butyric acid methyl ester fullerene or PCBM) have been found to be quite effective in delivering power conversion efficiencies up to 5%.[150−161] The morphology of the heterogeneous junction is very sensitive to the treatment procedure adopted during the film casting and annealing process. It has been proposed that an initial crystallization of P3HT chains, followed by diffusion of PCBM molecules to nucleation sites to form aggregates of PCBM is responsible for morphology evolution in these cells.[157,162,163] Local film structures with device performance have been mapped using photoconductive atomic force microscopy (pcAFM) with 20 nm resolution[148] and electrostatic force microscopy (EFM).[164] The schematic of the conductive-AFM set up to image the photocurrent distributions in organic thin films is shown in Figure 9.

The use of semiconductor nanocrystals in organic photovoltaic cells has been the focus of many recent research efforts.[159,166−172] The blend of polymer and CdSe quantum dots, for example, facilitates charge separation and the generation of photocurrents under visible light irradiation.[161] Blends of conjugated polymers and semiconductor nanoparticles have also been probed to investigate the photoinduced charge transfer processes.[170,171] Alivisatos and co-workers[165,169] have shown that CdSe nanorods, when combined with poly(3-hexylthiophene), create charge transfer junctions with high interfacial area (see for example Figure 10). These researchers succeeded in optimizing the overlap between the cell absorption and solar spectrum. By improving the polymer−semiconductor interface it should be possible to increase the carrier mobilities and hence the overall photoconversion efficiency. The details on the mechanism of photocurrent generation and recent advances in organic solar cells can be found in recent reviews.[149,152,153,155,160,161,173−176]

c. Quantum Dot Sensitized Solar Cells (QDSSC). As discussed in section B above, by coupling a short bandgap semiconductor such as CdSe with another semiconductor with favorable energetics, it is possible to maximize the efficiency of charge separation through charge rectification.[69] Suitable matching of the conduction and valence bands of the two semiconductors allows accumulation of electrons and holes in two separate particles, thus allowing enough time to capture one of the charge carriers at the electrode surface. For example, chemically or electrochemically deposited or self-assembled CdS and CdSe nanocrystallites have been shown to inject electrons into wider gap materials such as TiO_2,[41,49,177−187] SnO_2,[56,72,188] and ZnO.[70,189,190] This process is often referred to as type II mechanism, which is analogous to dye sensitization of semiconductor films, the dye being replaced by a short bandgap semiconductor (Figure 11). In a recent study nitrogen doped TiO_2 nanoparticle (TiO_2/N) films have been modified with CdSe quantum dots.[186] CdSe linked to TiO_2/N nanoparticles was found to increase the photocurrent and power conversion of the films compared to standard TiO_2/N films without quantum dot sensitization.

Short bandgap semiconductor quantum dots such as CdSe, InP, InAs, PbS, and PbSe with their tunable band edge offer new opportunities for harvesting light energy in the visible region of the solar spectrum.[32,45,51,108,191] Alvisatos and co-workers[192] fabricated planar donor−acceptor (D−A) heterojunctions by sequentially spin casting films of CdTe and then

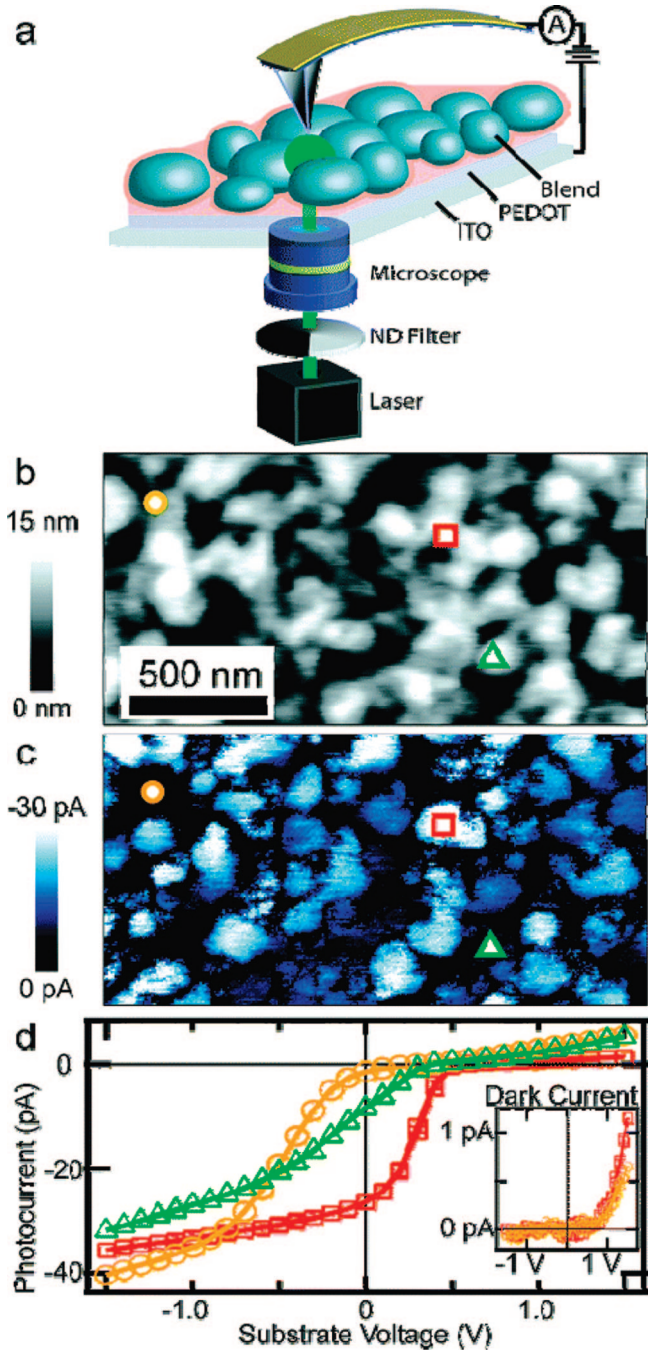

Figure 9. (a) Schematic of a conductive AFM set up to probe photovoltaic blend film. Current is collected with a metal-coated AFM tip. (b) AFM height image of an MDMO-PPV:PCBM 20:80 film spin-coated from xylenes. (c) Photocurrent map measured with zero external bias and an illumination intensity of $\sim 10^4$ W m^{-2} at 532 nm. (d) Local current−voltage data acquired at the three locations indicated in b and c. Inset: Local current−voltage data without illumination. (From ref 148.)

CdSe on indium tin oxide (ITO) glass. The photoaction spectrum revealed features from both the CdSe and CdTe absorption spectra, thus confirming the contributions from both components. External quantum efficiencies approaching 70% and power conversion efficiency of 2.9% were reported. Efficient quenching of photoluminescence and a reduced emission lifetime for CdTe nanocrystals support a spatial charge separation of the photoexcited electron−hole pairs due to tunneling of charge carriers through the thin organic layer between CdTe and CdSe nanocrystals.[193]

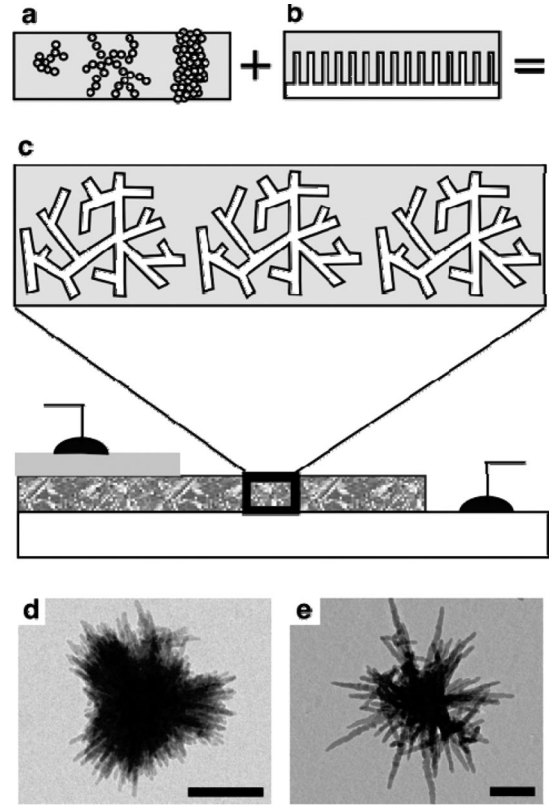

Figure 10. Hyperbranched nanocrystal solar cells (a) with the controlled morphology of templated approaches (b). Defects such as islands and aggregates detrimental to the performance of conventional spin-cast hybrid cells are eliminated in hyperbranched particle composites (c). The hyperbranched particles span the entire thickness of the active film, thereby enhancing electron transport. In panels (d) and (e), transmission electron micrographs show the 3-D structure of CdSe and CdTe hyperbranched nanocrystals, respectively. Scale bar, 100 nm. (From ref 165.)

In order to explore the salient features of quantum dots in photoelectrochemical cells, we assembled TiO_2 and CdSe nanoparticles using bifunctional surface modifiers of the type HS-R-COOH. Such an approach has been used to successfully link TiO_2 nanoparticles to CdS [136,194,195] as well as to gold nanoparticles.[135,196] In a typical procedure, OTE/TiO_2 electrode (optically transparent electrode modified with TiO_2 particulate film) is immersed in an acetonitrile solution of HOOC-R-SH (viz., mercaptopropionic acid) solution for 2−4 h.[49] The electrode after washing thoroughly with acetonitrile is then immersed in a toluene suspension of CdSe quantum dots. TiO_2 has a strong affinity for the carboxylate group of the linker molecules, as demonstrated previously with a variety of sensitizing dyes.[197,198] Thiol and amine groups, on the other hand, bind strongly to CdSe nanoparticles.[133,199−203] The coloration of the electrode confirms anchoring CdSe quantum dots onto a nanostructured TiO_2 film. Spin casting and electrophoretic deposition are also convenient methods to deposit films of CdSe quantum dots.[204−206] These electrodes can then be inserted into a photoelectrochemical cell for evaluating their photoresponse and I−V characteristics.

The absorption spectra of TiO_2 films following surface binding of four different sized CdSe quantum dots are shown in Figure 12. The absorption spectra of four different size CdSe particles anchored on TiO_2 particulate films and TiO_2 nanotubes which exhibit excitonic transitions at 580, 540, 520, and 505 nm are similar to the one observed in the solution spectra and correspond to diameter 2.3, 2.6, 3.0, and 3.7 nm. The size

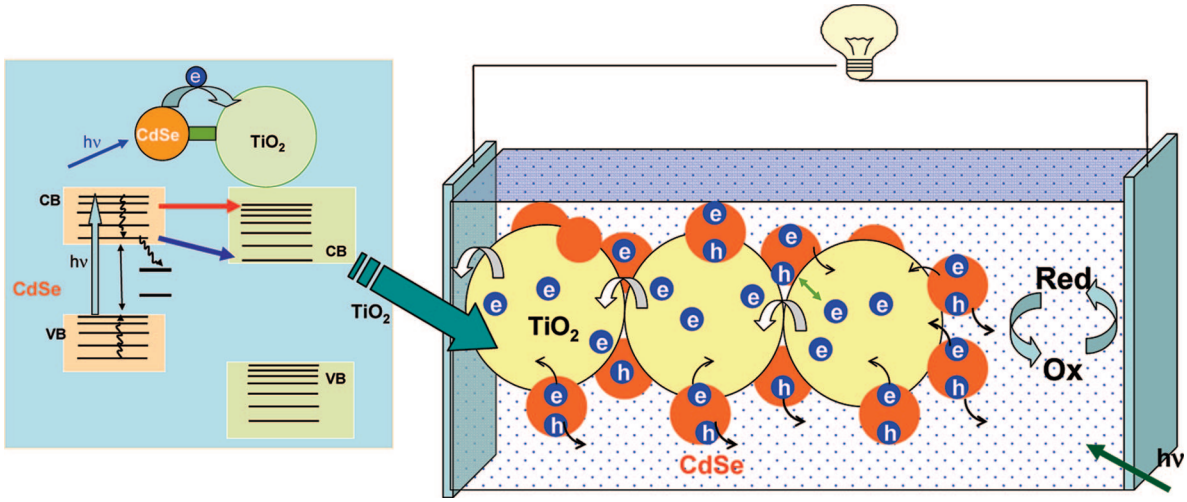

Figure 11. Principle of operation of quantum dot sensitized solar cell (QDSSC). Charge injection from excited CdSe quantum dots into TiO_2 nanoparticles is followed by collection of charges at the electrode surface. The redox electrolyte (e.g., sulfide/polysulfide) scavenges the holes and thus ensures regeneration of the CdSe.

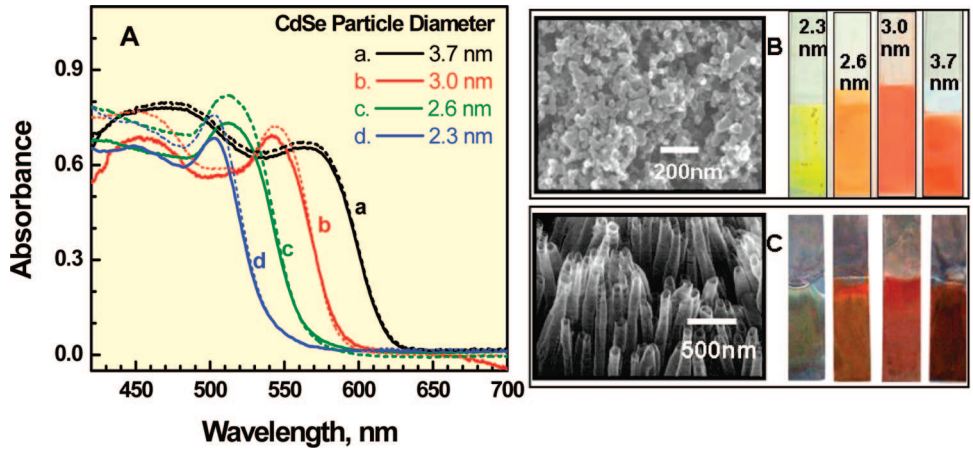

Figure 12. (A) Absorption spectra of (a) 3.7, (b) 3.0, (c) 2.6, and (d) 2.3 nm diameter CdSe quantum dots anchored on nanostructured TiO_2 films OTE/TiO_2(nanoparticle)/CdSe (solid lines) and Ti/TiO_2(nanotubes)/CdSe (dashed lines) The scanning electron micrographs (SEM) of TiO_2 particulate (B) and TiO_2 nanotube (C) films along with photographs of CdSe deposited TiO_2 films are also shown. (From ref 33.)

dependent coloration offers an opportunity to tune the coloration of the TiO_2 films and this in turn enables one to selectively modulate the absorption of incident light.

An important point that emerges from the absorption spectra is the fact that the native quantization property of CdSe nanocrystals is retained even after their binding to the TiO_2 surface. The ability to achieve relatively high coverage of CdSe quantum dots on TiO_2 surface shows the penetration of small size CdSe quantum dots into the porous network within the TiO_2 film and allows a uniform coverage throughout the film. Such monolayer coverage of the CdSe particles is analogous to the mesoscopic TiO_2 films modified with sensitizing dyes.

d. Size Dependent Photoelectrochemical Response. The photoelectrochemical response of OTE/TiO_2/CdSe films to monochromatic light irradiation can be analyzed in terms of incident photon to charge carrier efficiency (IPCE), also referred to as external quantum efficiency. IPCE was determined from short circuit photocurrents (J_{sc}) monitored at different excitation wavelengths (λ) using the expression

$$\mathrm{IPCE}\% = \frac{1240 \times J_{\mathrm{shortcircuit}}(\mathrm{A/cm^2})}{\lambda(\mathrm{nm}) \times I_{\mathrm{incident}}(\mathrm{W/cm^2})} \times 100\%$$

where I_{incident} is the power of energy of the monochromatic light incident on the electrode. The IPCE action spectra for OTE/TiO_2(NP)/CdSe and Ti/TiO_2(NT)/CdSe electrodes (NP and NT represent nanoparticle and nanotube films) are presented in Figure 13. The photocurrent action spectra obtained with 3.7, 3.0, 2.6, and 2.3 nm CdSe particles exhibit current peaks at 580, 540, 520, and 505 nm, which closely match the absorption plots in Figure 12. These observations confirm that the photocurrent generation at OTE/TiO_2(NP)/CdSe and Ti/TiO_2(NT)/CdSe electrodes originates from the individual CdSe quantum dots and that their size quantization property is responsible for tuning the performance of quantum dot solar cells.[33] In particular, the ability to modulate the photoresponse by varying the size of CdSe particles affords the possibility to tune the performance of quantum dot solar cells. Similar observation of band-edge tuning was reported for CdSe quantum dots[50] and bismuth sulfide quantum dots[47] adsorbed on TiO_2 particles.

Comparison of IPCE at the excitonic peaks shows an interesting dependence on the particle size. The higher IPCE values obtained with 2.3 and 2.6 nm CdSe quantum dots indicated that the smaller size particles are more energetic in their excited-state and are capable of injecting electrons into TiO_2 at a faster rate. Arguments have been made in the literature for injection of hot electrons from the quantized semiconductor particles.[34,207] Careful analysis of the ultrafast kinetic measure-

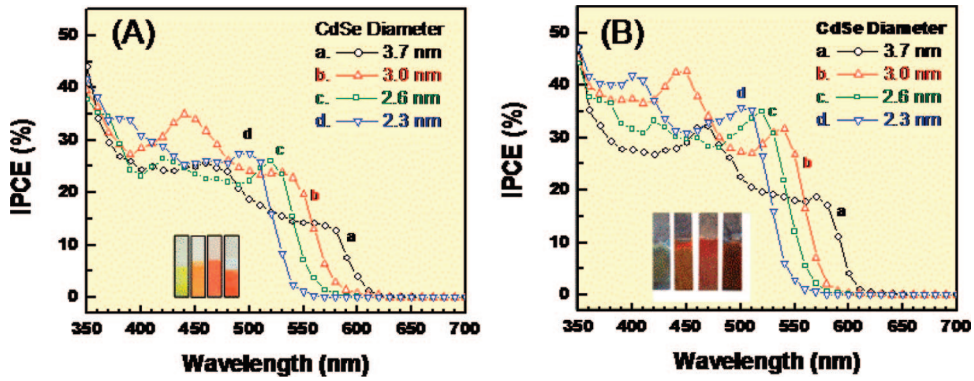

Figure 13. Photocurrent action spectra recorded in terms of Incident photon to charge carrier generation efficiency (IPCE) of (A) OTE/TiO_2(NP)/CdSe and (B) Ti/TiO_2(NT)/CdSe electrodes (electrodes are shown in the inset). The individual IPCE responses correspond to (a) 3.7, (b) 3.0, (c) 2.6, and (d) 2.3 nm diameter CdSe quantum dots anchored on nanostructured TiO_2 films. 0.1 M Na_2S solution was used as redox electrolyte. (From ref 33.)

ments needs to be pursued to establish the contribution of hot electron injection in such systems.

It is also interesting to note that the maximum IPCE obtained with CdSe quantum dots linked to TiO_2 particles and tubes are different. The maximum IPCE values in the visible region (Figure 13) range from 25% to 35% for OTE/TiO_2(NP)/CdSe electrodes while they vary from 35% to 45% for OTE/Ti/TiO_2(NT)/CdSe electrodes. These IPCE values are relatively higher than those reported in the literature for the sensitization of TiO_2 films (IPCE 25%)[208] and ZnO nanorods (IPCE = 18%)[209] with CdSe quantum dots.[208] Higher power conversion efficiency has also been reported by Toyoda and co-workers using TiO_2 inverse opal structures[210] and coating with ZnS.[211] Other studies have also observed enhancement in photocurrent response using TiO_2 nanotubes,[187,212,213] nanowires,[212] and nanobelts.[214] High external quantum efficiencies (>70%) in ferro-/ferricyanide solutions have been obtained for ZnO/CdSe core−shell nanowire arrays annealed at 400 °C.[190] Structural transition in nanocrystalline CdSe nanowire shell, from cubic zinc blende to hexagonal wurtzite structure seems to play an important role in enhancing photocurrent generation. These results demonstrate the necessity of optimizing nanostructure assemblies in an orderly fashion.

The maximum photocurrents obtained with 3.0 nm CdSe particles were 2.0 and 2.4 mA/cm^2 for OTE/TiO_2(NP)/CdSe and Ti/TiO_2(NT)/CdSe electrodes respectively under visible light irradiation (λ > 420 nm, 80 mW/cm^2). The open-circuit photovoltage for these two electrodes using Na_2S redox electrolyte and Pt as counter electrode were 600 and 580 mV respectively. The fill factor for these photoelectrochemical cells was estimated as ~0.4. We estimated the overall power conversion efficiency as 0.6% and 0.7% for OTE/TiO_2(NP)/CdSe and Ti/TiO_2(NT)/CdSe electrodes respectively. In a recent study, an overall conversion efficiency of over 1.7% at 0.1 sun and 1% at full sun intensity with a cobalt(II/III)-based redox system was reported for CdSe sensitized TiO_2 solar cells.[50]

Two opposing effects dictate the overall photocurrent generation at OTE/TiO_2/CdSe electrodes. Decreasing particle size has a favorable effect as the shift in conduction band to negative potentials favors the charge injection processes by increasing the driving force. The increase in the photocurrent seen with 3.7 and 3.0 nm diameter CdSe particles supports this argument. On the other hand decreasing particle size results in the absorption blue-shift and thus causes relatively poor absorption of incident visible photons (e.g., 2.3 nm diameter particles harvest less visible photons than 3.0 nm diameter particles).

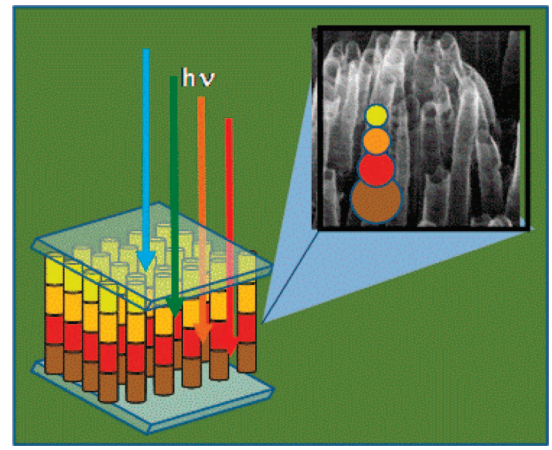

Figure 14. Artistic impression of a rainbow solar cell assembled with different size CdSe quantum dots on TiO_2 nanotube array. (From ref 33.)

Since smaller semiconductor quantum dots exhibit higher photoconversion efficiency but absorb less lower energy photons than larger size particles we can anchor the quantized particles on a nanotube array to maximize the capture of the incident light while collecting and transmitting electrons through the TiO_2 tube network (Figure 14). It is true that the excess energy of electrons of small size particles is lost once they are transferred to the TiO_2 manifold. Such a rainbow cell configuration, however, allows one to couple the faster electron injection rate of small size particles and greater absorption range of large particles effectively.

E. Emerging Strategies to Capture and Transport Photogenerated Electrons

Fast capture of electrons at the quantum dot interface remains a major challenge for efficient harvesting of light energy. Such an issue is of great importance if one is interested in exploiting multiple charge carrier generation for photocurrent generation. The strategy of encapsulating CdSe quantum dots with an electron acceptor shell or decorating on a semiconductor nanotube assembly can provide new ways to enhance the capture and transport of photogenerated electrons. Figure 15 illustrates two strategies to develop carbon nanostructure-semiconductor nanocrystal based light harvesting assemblies.

a. Fullerene Clusters As Electron Acceptors. Fullerenes exhibit rich photochemistry and act as electron shuttles in photochemical solar cells.[215] They also play an important role

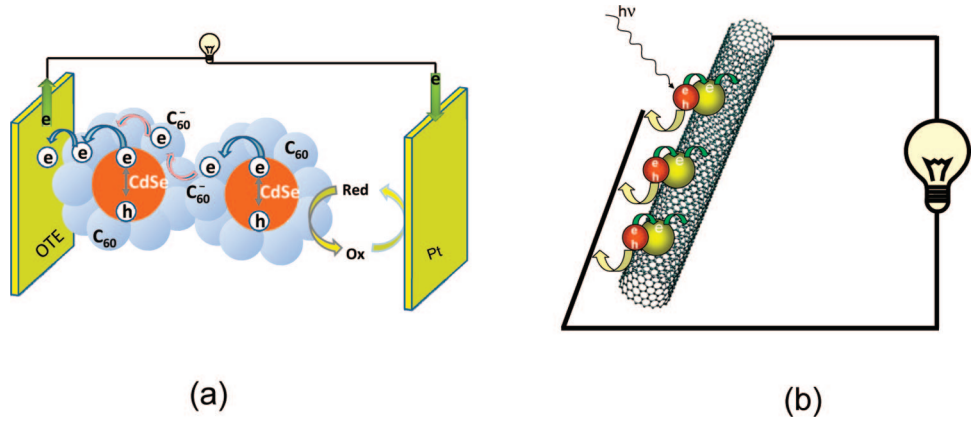

Figure 15. Photocurrent generation using (a) CdSe-nC_{60} composite clusters and (b) single wall carbon nanotubes.

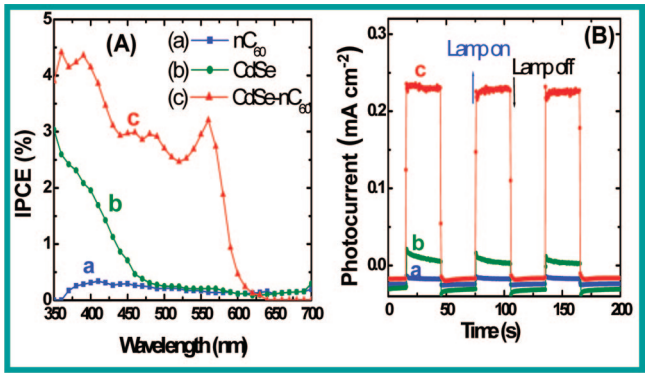

Figure 16. (A) Dependence of incident photon to current generation efficiency (IPCE) on the incident wavelength and (B) the photocurrent response of the electrodes to ON-OFF cycles of illumination. (a) nC_{60}, (b) CdSe quantum dots, and (c) CdSe−*n*C_{60} clusters on SnO_2 film electrodes. The electrolyte was 0.1 M Na_2S in water. (From ref 206.)

in improving the performance of organic photovoltaic cells.[216−218] C_{60} and its derivatives are widely used to capture and transport electrons in organic solar cells.[149,219−221] The electron accepting property of fullerenes has also been utilized for photocurrent generation in porphyrene-C_{60} based cluster films.[222] It would be interesting to see whether C_{60} can be effective for harvesting electrons from photoexcited CdSe quantum dots. In a previous study effort was made to dropcast CdSe quantum dots and C_{60} mixture on a conducting surface for the purpose of demonstrating photovoltaic performance.[223] The poor interaction between the two components resulted in relatively lower photocurrent generation. A new approach of capping the CdSe quantum dots with a molecular shell of electron acceptor C_{60} was attempted recently to improve the capture of photogenerated electrons in quantum dots in a photoelectrochemical cell.[206] A similar approach of capturing photogenerated electrons from CdSe quantum dots with different electron acceptors has been demonstrated by spectroscopic methods.[224]

CdSe and CdSe−*n*C_{60} clusters were directly deposited as films from quantum dots and clusters dispersed in an acetonitrile: toluene (4:1) mixed solvent. Figure 16A shows the photocurrent action spectra presented in terms of incident charge carrier generation efficiency (IPCE) at different excitation wavelengths. Both CdSe and CdSe−*n*C_{60} electrodes show an onset of photocurrent generation at 600 nm matching the onset of CdSe absorption. The maximum open circuit photovoltage and photocurrent observed with white light illumination (λ > 300 nm, incident light 100 mW/cm^2) were 0.3 V and 0.25 mA/cm^2, respectively. The observed photocurrents were 2−3 orders of magnitude greater than the one obtained with dropcast films of CdSe and C_{60}.[223] Figure 16B shows the reproducibility and stability of the photocurrent response of these films. The Na_2S electrolyte scavenges the holes from CdSe thus enabling the regeneration of the CdSe in the film.[49] The IPCE response of CdSe-nC_{60} is not a simple additive effect arising from individual components, but reflects the synergy arising from the excited interaction between CdSe and *n*C_{60}. Since nC_{60} is a good electron acceptor (E^0 = −0.2 V vs NHE) one expects a quick electron transfer from excited CdSe into *n*C_{60}. The electron stabilization in *n*C_{60} clusters and its ability to generate photocurrent are described in an earlier study.[216,222,225,226] The C_{60} anion stabilized within the cluster is able to transport electrons to the collecting electrode surface. Figure 15a illustrates the photoinduced electron transfer between CdSe and C_{60} followed by the electron transport through the C_{60} network to the collecting surface of OTE, which is previously coated with SnO_2 nanoparticles. In addition, coupling of semiconductor quantum dots with sensitizing dyes (e.g., Ru−polypyridine complexes) to promote energy and/or electron transfer can provide new ways to harvest a wider spectrum of incident light energy.[114,224,227]

b. Carbon Nanotubes as Conduits for Charge Transport. Unique electrical and electronic properties, wide electrochemical stability window, and high surface area have prompted many researchers to employ carbon nanostructures such as single wall carbon nanotube (SWCNT) assemblies for energy conversion devices.[228−230] The photon harvesting property of carbon nanotubes has been discussed in detail in recent review articles.[231,232] The use of a nanotube support to anchor semiconductor particles provides a convenient way to capture photogenerated charge and transport them to the electrode surface. Efforts to synthesize semiconductor-CNT composite films have shown significant progress in recent years.[233−241] Early studies mainly focused on establishing synthetic strategies and characterization of the composite systems. These include carbon nanotubes in contact with TiO_2,[242,243] SnO_2,[244] ZnO,[245] CdSe,[237,239,246] CdS,[234,247−249] CdSe/pyrene,[250] and CdS/TiO_2.[249]

Of particular interest is the semiconductor−CNT composite that is capable of generating photocurrent from visible light with unusually high efficiency.[234,248] Excited state interaction between TiO_2,[251−254] ZnO,[245] and CdS[234,248,249] and carbon nanotubes has been investigated in detail by monitoring the luminescence quenching or by Fermi-level equilibration. Excitation of CdS deposited on SWCNT films produced photocurrent with a maximum incident photon to current generation efficiency of 0.5% and thus provides evidence for the electron transfer pathway in the composite. The ability of the CdS-SWCNT

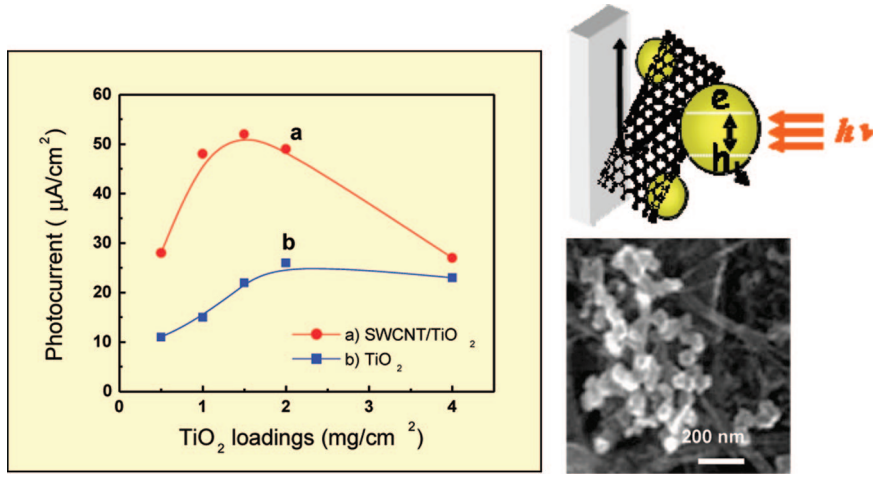

Figure 17. Left: Photocurrent response as a function of the amount of TiO_2 deposited on carbon fiber electrode (CFE): (a) In the presence and (b) absence of SWCNT scaffold. SWCNT concentration was maintained constant at 0.2 mg/cm^2 while TiO_2 loading was varied. Right: Scheme showing the electron transport through SWCNT and SEM image of the SWCNT−TiO_2 composite. (From ref 251.)

nanocomposite system to undergo photoinduced charge separation opens up new ways to design light harvesting assemblies.

The role of SWCNT in enhancing the photoelectrochemical performance of TiO_2 film can be probed by varying the ratio of TiO_2/SWCNT in the composite film. A commercially available TiO_2 (Degussa P-25) suspension in water was drop cast on carbon fiber electrode (CFE) with and without SWCNT. Figure 17 compares the photocurrent observed with CFE/TiO_2 and CFE/SWCNT/TiO_2 electrodes at different loading of TiO_2 particles. In the case of the CFE/TiO_2 film, we observe an increase in photocurrent with increased TiO_2 loading (at loadings below 2 mg/cm^2) as more of the excited TiO_2 particles undergo charge separation and participate in the photocurrent generation. At higher TiO_2 loadings we observe saturation in the photocurrent showing the limitations of light absorption within the TiO_2 film. It is interesting to note that the photocurrent observed at these TiO_2 loadings with SWCNT support is significantly greater than the photocurrent observed without the SWCNT support. The usefulness of SWCNT support architecture in improving the photocurrent generation in TiO_2 based photoelectrochemical solar cells is discussed elsewhere.[251,255] Two dimensional carbon nanostructures such as graphene sheets offer new ways to disperse semiconductor and metal nanoparticles.[256,257] Utilization of such nanocomposites in energy conversion devices has yet to be tested for the effectiveness of graphene as a support carbon nanomat.

c. Nanowire and Nanotube Array Based Solar Cells. Semiconductor nanowires with high aspect ratio are now being grown as vertically aligned arrays on electrode surfaces to increase the light absorption and to facilitate efficient radial collection of carriers.[258,259] Most of the recent studies have focused on the utilization of ZnO,[190,209,260] SnO_2,[188] and TiO_2 nanowires.[261] The 1-D array of these large bandgap semiconductors can be readily modified with CdS or CdSe quantum dots for extending the photoresponse into the visible.[33,209,262] The operation of TiO_2 nanotube array based semiconductor cells has already been discussed in the earlier section. By comparing the behavior of nanorod array and planar Si[263] and Cd(Se, Te)[264] photoelectrodes Spurgeon et al. concluded that the fill factors of the nanorod array photoelectrodes were generally superior to those of the planar junction devices.

Silicon nanowires are emerging as another class of light harvesting semiconductors.[264−269] If semiconductor nanorods having radial p-n junctions are arranged in a vertically aligned

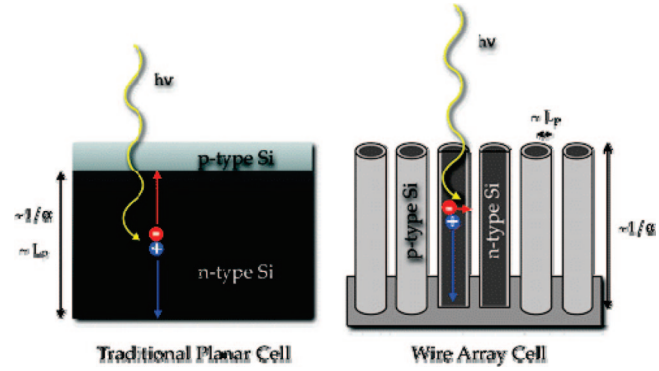

Figure 18. Schematic drawing of the difference between a traditional planar solar cell and a wire array solar cell. In the planar cell, the minority carrier diffusion length (L_p) must be comparable to the absorption length ($1/\alpha$). In the wire array cell, the minority carriers can diffuse radially to the junction, while light is still absorbed along the axial dimension of the wire. (From ref 263.)

array, the light can be absorbed along the long axis of the rod and the charge carriers can diffuse a short distance radially to the junction (Figure 18).[263] Such electrodes have been shown to exhibit significantly higher photocurrent than the control Si electrode during the operation of a photoelectrochemical solar cell. Silicon nanowires grown on Si(111)/Au substrates were controllably p-type doped by addition of tri-Me boron. These p-Si nanowire arrays gave a photovoltage of 220 mV in $[Ru(bpy)_3]^{2+}$ solution when illuminated by white light.[270] Coaxial silicon nanowire solar cells based on p-type/intrinsic/n-type (p-i-n) elements yield a maximum power output of up to 200 pW per nanowire device and an apparent energy conversion efficiency of up to 3.4% under one solar equivalent (1-sun) illumination.[271] Such interconnected p-i-n silicon nanowire based photovoltaic elements have been projected as the potential nanopower sources to drive functional nanoelectronic sensors and logic gates. Scanning photocurrent microscopy of single Si nanowire devices has indicated the minority carrier diffusion lengths of 2.2 μm.[271] Efforts are being made in several research groups to obtain fundamental understanding of charge separation and recombination processes in semiconductor nanowires [272−280]

F. Concluding Remarks

The orphan status of solar energy as a major source of our energy chain is expected to change as the demand for clean

energy increases. During the last two decades significant advances have been made in designing photoactive nanostructure architectures and inorganic−organic hybrid assemblies. Many of the newly synthesized nanomaterials hold the promise of being able to meet the global challenge of supplying clean energy. Quantum dot and carbon nanostructure based solar cells are still in their infancy. The recent advances in utilizing quantum dots or semiconductor nanocrystals as light energy harvesters provide unique opportunities for the development of next generation solar cells. Developing new and revolutionary viable strategies to organize ordered assemblies on electrode surfaces will be the key to improving the performance of quantum dot solar cells. Commercialization of large scale solar cells based on nanostructure architecture has yet to be realized. With the recent surge in interest of renewable energy we can expect major breakthroughs in developing economically viable solar energy conversion devices in the near future.

Acknowledgment. The research at Notre Dame Radiation Laboratory is supported by the Office of Basic Energy Sciences of the U.S. Department of Energy. Thanks are due to the students, postdoctoral associates, visiting scientists and collaborators who have actively contributed to the significant advance of our solar energy research. (See http://www.nd.edu/~pkamat for further details.) Individual contributions are recognized in the cited work. This is contribution NDRL 4770 from the Notre Dame Radiation Laboratory.

References and Notes

(1) Kamat, P. V. Meeting the Clean Energy Demand: Nanostructure Architectures for Solar Energy Conversion. *J. Phys. Chem. C* **2007**, *111*, 2834–2860.

(2) Green, M. A. *Third Generation Photovoltaics: Advanced Solar Energy Conversion*; Springer-Verlag: Berlin, Germany, 2004.

(3) Barnham, K. W. J.; Mazzer, M.; Clive, B. Resolving the energy crisis:nuclear or photovoltaics. *Nat. Mater.* **2006**, *5*, 161–164.

(4) Meyer, G. J. Molecular Approaches to Solar Energy Conversion with Coordination Compounds Anchored to Semiconductor Surfaces. *Inorg. Chem.* **2005**, *44*, 6852–6864.

(5) Henglein, A. Small-particle research: Physicochemical properties of extremely small colloidal metal and semiconductor particles. *Chem. Rev.* **1989**, *89*, 1861–73.

(6) Steigerwald, M. L.; Brus, L. E. Semiconductor crystallites: A class of large molecules. *Acc. Chem. Res.* **1990**, *23*, 183–8.

(7) Brus, L. Electronic wave functions in semiconductor clusters: Experiment and theory. *J. Phys. Chem.* **1986**, *90*, 2555–60.

(8) Weller, H. Quantized semiconductor particles: A novel state of matter for materials science. *Adv. Mater.* **1993**, *5*, 88–95.

(9) Banyai, L.; Koch, S. W. *Semiconductor quantum Dots*; World Scientific Publishing Co.: River Edge, NJ, 1993.

(10) Kamat, P. V. Native and surface modified semiconductor nanoclusters. In *Molecular level artificial photosynthetic materials. Progress in Inorganic Chemistry Series*; Meyer, J., Ed.; John Wiley & Sons, Inc.: New York, 1997; pp 273−243.

(11) Alivisatos, P. Perspectives on the physical chemistry of semiconductor nanocrystals. *J. Phys. Chem.* **1996**, *100*, 13226–13239.

(12) Kamat, P. V. Photophysical, photochemical and photocatalytic aspects of metal nanoparticles. *J. Phys. Chem. B* **2002**, *106*, 7729–7744.

(13) Thomas, K. G.; Kamat, P. V. Chromophore Functionalized Gold Nanoparticles. *Acc. Chem. Res.* **2003**, *36*, 888–898.

(14) Mulvaney, P.; Liz-Marzan, L. M.; Giersig, M.; Ung, T. M. Silica encapsulation of quantum dots and metal clusters. *J. Mater. Chem.* **2000**, *10*, 1259–1270.

(15) Liz-Marzan, L. M.; Mulvaney, P. The assembly of coated nanocrystal. *J. Phys. Chem. B* **2003**, *107*, 7312–7326.

(16) Perez-Juste, J.; Pastoriza-Santos, I.; Liz-Marzan, L. M.; Mulvaney, P. Gold nanorods: Synthesis, characterization and applications. *Coord. Chem. Rev.* **2005**, *249*, 1870–1901.

(17) Grieve, K.; Mulvaney, P.; Grieser, F. Synthesis and electronic properties of semiconductor nanoparticles/quantum dots. *Curr. Opin. Colloid Interface Sci.* **2000**, *5*, 168–172.

(18) Ouyang, M.; Huang, J. L.; Lieber, C. M. Fundamental electronic properties and applications of single-walled carbon nanotubes. *Acc. Chem. Res.* **2002**, *35*, 1018–1025.

(19) Xia, Y. N.; Yang, P. D.; Sun, Y. G.; Wu, Y. Y.; Mayers, B.; Gates, B.; Yin, Y. D.; Kim, F.; Yan, Y. Q. One-dimensional nanostructures: Synthesis, characterization, and applications. *Adv. Mater.* **2003**, *15*, 353–389.

(20) El-Sayed, M. A. Some interesting properties of metals confined in time and nanometer space of different shapes. *Acc. Chem. Res.* **2001**, *34*, 257–264.

(21) Kelly, K. L.; Coronado, E.; Zhao, L. L.; Schatz, G. C. The Optical Properties of Metal Nanoparticles: The Influence of Size, Shape, and Dielectric Environment. *J. Phys. Chem. B* **2003**, *107*, 668–677.

(22) Burda, C.; Chen, X. B.; Narayanan, R.; El-Sayed, M. A. Chemistry and properties of nanocrystals of different shapes. *Chem. Rev.* **2005**, *105*, 1025–1102.

(23) Sirbuly, D. J.; Law, M.; Yan, H.; Yang, P. Semiconductor Nanowires for Subwavelength Photonics Integration. *J. Phys. Chem. B* **2005**, *109*, 15190–15213.

(24) Cao, G. Growth of Oxide Nanorod Arrays through Sol Electrophoretic Deposition. *J. Phys. Chem. B* **2004**, *108*, 19921–19931.

(25) Jin, R.; Cao, Y. C.; Hao, E.; Metraux, G. S.; Schatz, G. C.; Mirkin, C. A. Controlling anisotropic nanoparticle growth through plasmon excitation. *Nature* **2003**, *425*, 487.

(26) Henzie, J.; Shuford, K. L.; Kwak, E. S; Schatz, G. C.; Odom, T. W. Manipulating the Optical Properties of Pyramidal Nanoparticle Arrays. *J. Phys. Chem. B* **2006**, *110*, 14028–14031.

(27) Murphy, C. J.; Gole, A. M.; Hunyadi, S. E.; Orendorff, C. J. One-Dimensional Colloidal Gold and Silver Nanostructures. *Inorg. Chem.* **2006**, *45*, 7544–7554.

(28) Wang, F.; Dong, A.; Sun, J.; Tang, R.; Yu, H.; Buhro, W. E. Solution-Liquid-Solid Growth of Semiconductor Nanowires. *Inorg. Chem.* **2006**, *45*, 7511–7521.

(29) Greene, L. E.; Yuhas, B. D.; Law, M.; Zitoun, D.; Yang, P. Solution-Grown Zinc Oxide Nanowires. *Inorg. Chem.* **2006**, *45*, 7535–7543.

(30) Kline, T. R.; Tian, M.; Wang, J.; Sen, A.; Chan, M. W. H.; Mallouk, T. E. Template-Grown Metal Nanowires. *Inorg. Chem.* **2006**, *45*, 7555–7565.

(31) Shockley, W.; Queisser, H. J. Detailed Balance Limit of Efficiency of p-n Junction Solar Cells. *J. Appl. Phys.* **1961**, *32*, 510–519.

(32) Nozik, A. J. Quantum dot solar cells. *Phys. E* **2002**, *14*, 115–120.

(33) Kongkanand, A.; Tvrdy, K.; Takechi, K.; Kuno, M. K.; Kamat, P. V. Quantum Dot Solar Cells. Tuning Photoresponse through Size and Shape Control of CdSe-TiO_2 Architecture. *J. Am. Chem. Soc.* **2008**, *130*, 4007–4015.

(34) Ross, R. T.; Nozik, A. J. Efficiency of hot-carrier solar energy converters. *J. Appl. Phys.* **1982**, *53*, 3813–8.

(35) Schaller, R. D.; Klimov, V. I. High Efficiency Carrier Multiplication in PbSe Nanocrystals: Implications for Solar Energy Conversion. *Phys. Rev. Lett.* **2004**, *92*, 186601.

(36) Schaller, R. D.; Agranovich, V. M.; Klimov, V. C. High-efficiency carrier multiplication through direct photogeneration of multi-excitons via virtual single-exciton states. *Nat. Phys.* **2005**, *1*, 189–195.

(37) Ellingson, R. J.; Beard, M. C.; Johnson, J. C.; Yu, P. R.; Micic, O. I.; Nozik, A. J.; Shabaev, A.; Efros, A. L. Highly efficient multiple exciton generation in colloidal PbSe and PbS quantum dots. *Nano Lett.* **2005**, *5*, 865–871.

(38) Califano, M.; Zunger, A.; Franceschetti, A. Efficient inverse Auger recombination at threshold in CdSe nanocrystals. *Nano Lett.* **2004**, *4*, 525–531.

(39) Kamat, P. V. Photochemistry on nonreactive and reactive (semiconductor) surfaces. *Chem. Rev.* **1993**, *93*, 267–300.

(40) Kamat, P. V., Meisel, D., Eds.; *Semiconductor Nanoclusters-Physical, Chemical and Catalytic Aspects. Studies in Surface Science and Catalysis*; Elsevier Science: Amsterdam, 1997; p 474.

(41) Gerischer, H.; Luebke, M. A particle size effect in the sensitization of TiO_2 electrodes by a CdS deposit. *J. Electroanal. Chem.* **1986**, *204*, 225–7.

(42) Vogel, R.; Pohl, K.; Weller, H. Sensitization of highly porous, polycrystalline TiO_2 electrodes by quantum sized CdS. *Chem. Phys. Lett.* **1990**, *174*, 241–6.

(43) Kohtani, S.; Kudo, A.; Sakata, T. Spectral sensitization of a TiO_2 semiconductor electrode by CdS microcrystals and its photoelectrochemical properties. *Chem. Phys. Lett.* **1993**, *206*, 166–70.

(44) Vogel, R.; Hoyer, P.; Weller, H. Quantum-sized PbS, CdS, Ag_2S, Sb_2S_3, and Bi_2S_3 particles as sensitizers for various nanoporous wide-bandgap semiconductors. *J. Phys. Chem.* **1994**, *98*, 3183–3188.

(45) Plass, R.; Pelet, S.; Krueger, J.; Gratzel, M.; Bach, U. Quantum dot sensitization of organic-inorganic hybrid solar cells. *J. Phys. Chem. B* **2002**, *106*, 7578–7580.

(46) Saurez, R.; Nair, P. K.; Kamat, P. V. Photoelectrochemical behavior of Bi_2S_3 nanoclusters and nanostructured thin films. *Langmuir* **1998**, *14*, 3236–3241.

(47) Peter, L. M.; Wijayantha, K. G. U.; Riley, D. J.; Waggett, J. P. Band-edge tuning in self-assembled layers of Bi_2S_3 nanoparticles used to photosensitize nanocrystalline TiO_2. *J. Phys. Chem. B* **2003**, *107*, 8378–8381.

(48) Liu, D.; Kamat, P. V. Photoelectrochemical behavior of thin CdSe and coupled TiO_2/CdSe semiconductor films. *J. Phys. Chem.* **1993**, *97*, 10769–73.

(49) Robel, I.; Subramanian, V.; Kuno, M.; Kamat, P. V. Quantum Dot Solar Cells. Harvesting Light Energy with CdSe Nanocrystals Molecularly Linked to Mesoscopic TiO_2 Films. *J. Am. Chem. Soc.* **2006**, *128*, 2385–2393.

(50) Lee, H. J.; Yum, J.-H.; Leventis, H. C.; Zakeeruddin, S. M.; Haque, S. A.; Chen, P.; Seok, S. I.; Grätzel, M.; Nazeeruddin, M. K. CdSe Quantum Dot-Sensitized Solar Cells Exceeding Efficiency 1% at Full-Sun Intensity. *J. Phys. Chem. C* **2008**, *112*, 11600–11608.

(51) Zaban, A.; Micic, O. I.; Gregg, B. A.; Nozik, A. J. Photosensitization of nanoporous TiO_2 Electrodes with InP Quantum Dots. *Langmuir* **1998**, *14*, 3153–3156.

(52) Gopidas, K. R.; Bohorquez, M.; Kamat, P. V. Photoelectrochemistry in semiconductor particulate systems. 16. Photophysical and photochemical aspects of coupled semiconductors. Charge-transfer processes in colloidal CdS−TiO_2 and CdS−AgI systems. *J. Phys. Chem.* **1990**, *94*, 6435–40.

(53) Vinodgopal, K.; Kamat, P. V. Enhanced rates of photocatalytic degradation of an azo dye using SnO_2/TiO_2 coupled semiconductor thin films. *Environ. Sci. Technol.* **1995**, *29*, 841–845.

(54) Bedja, I.; Kamat, P. V. Capped semiconductor colloids. Synthesis and Photoelectrochemical properties of TiO_2 capped SnO_2 surfaces. *J. Phys. Chem.* **1995**, *99*, 9182–9188.

(55) Vinodgopal, K.; Bedja, I.; Kamat, P. V. Nanostructured semiconductor films for photocatalysis. Photoelectrochemical behavior of SnO_2/TiO_2 coupled systems and its role in photocatalytic degradation of a textile azo dye. *Chem. Mater.* **1996**, *8*, 2180–2187.

(56) Nasr, C.; Hotchandani, S.; Kim, W. Y.; Schmehl, R. H.; Kamat, P. V. Photoelectrochemistry of composite semiconductor thin films. Photosensitization of SnO_2/CdS coupled nanocrystallites with a Ruthenium complex. *J. Phys. Chem. B* **1997**, *101*, 7480–7487.

(57) Sant, P. A.; Kamat, P. V. Inter-Particle Electron Transfer between Size-Quantized CdS and TiO_2 Semiconductor Nanoclusters. *Phys. Chem. Chem. Phys.* **2002**, *4*, 198–203.

(58) Spanhel, L.; Weller, H.; Henglein, A. Photochemistry of semiconductor colloids. 22. Electron injection from illuminated CdS into attached TiO_2 and ZnO particles. *J. Am. Chem. Soc.* **1987**, *109*, 6632–5.

(59) Spanhel, L.; Henglein, A.; Weller, H. Photochemistry of colloidal semiconductors. 24. Interparticle electron transfer in Cd_3P_2−TiO_2 and Cd_3P_2−ZnO sandwich structures. *Ber. Bunsen-Ges. Phys. Chem.* **1987**, *91*, 1359–63.

(60) Dabbousi, B. O.; RodriguezViejo, J.; Mikulec, F. V.; Heine, J. R.; Mattoussi, H.; Ober, R.; Jensen, K. F.; Bawendi, M. G. (CdSe)ZnS core-shell quantum dots: Synthesis and characterization of a size series of highly luminescent nanocrystallites. *J. Phys. Chem. B* **1997**, *101*, 9463–9475.

(61) Tian, Y.; Newton, T.; Kotov, N. A.; Guldi, D. M.; Fendler, J. H. Coupled Composite CdS-CdSe and Core-Shell Types of (CdS)CdSe and (CdSe)CdS Nanoparticles. *J. Phys. Chem.* **1996**, *100*, 8927–8939.

(62) Mews, A.; Kadavanich, A. V.; Banin, U.; Alivisatos, A. P. Structural and spectroscopic characterization of the CdS/HgS/CdS quantum dot quantum wells. *Phys. Rev. B* **1996**, *53*, 13242–13245.

(63) Micic, O. I.; Smith, B. B.; Nozik, A. J. Core-Shell Quantum Dots of Lattice-Matched $ZnCdSe_2$ Shells on InP Cores: Experiment and Theory. *J. Phys. Chem. B* **2000**, *104*, 12149–12156.

(64) Willner, I.; Eichen, Y. TiO_2 and CdS colloids stabilized by beta-cyclodextrins: Tailored semiconductor-receptor systems as a means to control interfacial electron-transfer processes. *J. Am. Chem. Soc.* **1987**, *109*, 6862–3.

(65) Henglein, A. Physicochemical properties of small metal particles in solution: "Microelectrode" reactions, chemisorption, composite metal particles, and the atom-to-metal transition. *J. Phys. Chem.* **1993**, *97*, 5457–71.

(66) Kamat, P. V. *Composite Semiconductor Nanoclusters, in Semiconductor Nanoclusters - Physical, Chemical and Catalytic Aspects*; Kamat, P. V., Meisel, D., Eds.; Elsevier Science: Amsterdam,1997; pp 237−259.

(67) Kamat, P. V. Photoinduced Transformations in Semiconductor-Metal Nanocomposite Assemblies. *Pure Appl. Chem.* **2002**, *74*, 1693–1706.

(68) Rajeshwar, K.; de Tacconi, N. R.; Chenthamarakshan, C. R. Semiconductor-Based Composite Materials: Preparation, Properties, and Performance. *Chem. Mater.* **2001**, *13*, 2765–2782.

(69) Liu, D.; Kamat, P. V. Electrochemical rectification in CdSe + TiO_2 coupled semiconductor films. *J. Electroanal. Chem. Interfacial Electrochem.* **1993**, *347*, 451–6.

(70) Hotchandani, S.; Kamat, P. V. Charge-transfer processes in coupled semiconductor systems. Photochemistry and photoelectrochemistry of the colloidal CdS−ZnO system. *J. Phys. Chem.* **1992**, *96*, 6834–9.

(71) Nasr, C.; Hotchandani, S.; Kamat, P. V. Photoelectrochemistry of composite semiconductor thin films. II. Photosensitization of SnO_2/TiO_2 coupled system with a ruthenium polypyridyl complex. *J. Phys. Chem. B* **1998**, *102*, 10047–10056.

(72) Nasr, C.; Kamat, P. V.; Hotchandani, S. Photoelectrochemical behavior of coupled SnO_2/CdSe nanocrystalline semiconductor films. *J. Electroanal. Chem.* **1997**, *420*, 201–207.

(73) Zhang, J. Z.; O'Neil, R. H.; Roberti, T. W. Femtosecond studies of interfacial electron-hole recombination in aqueous CdS colloids. *Appl. Phys. Lett.* **1994**, *64*, 1989–1991.

(74) Nirmal, M.; Brus, L. Luminescence photophysics in semiconductor nanocrystals. *Acc. Chem. Res.* **1999**, *32*, 407–414.

(75) Empedocles, S.; Bawendi, M. Spectroscopy of Single CdSe Nanocrystallites. *Acc. Chem. Res.* **1999**, *32*, 389–396.

(76) Kuno, M.; Fromm, D. P.; Hamann, H. F.; Gallagher, A.; Nesbitt, D. J. Nonexponential "blinking" kinetics of single CdSe quantum dots: A universal power law behavior. *J. Chem. Phys.* **2000**, *112*, 3117–3120.

(77) Halpert, J. E.; Porter, V. J.; Zimmer, J. P.; Bawendi, M. G. Synthesis of CdSe/CdTe Nanobarbells. *J. Am. Chem. Soc.* **2006**, *128*, 12590–12591.

(78) Chan, W. C. W.; Nie, S. Quantum Dot Bioconjugates for Ultrasensitive Nonisotopic Detection. *Science* **1998**, *281*, 2016–2018.

(79) Mattoussi, H.; Mauro, J. M.; Goldman, E. R.; Anderson, G. P.; Sundar, V. C.; Mikulec, F. V.; Bawendi, M. G. Self-assembly of CdSe-ZnS quantum dot bioconjugates using an engineered recombinant protein. *J. Am. Chem. Soc.* **2000**, *122*, 12142–12150.

(80) Niemeyer, C. M. Nanoparticles, Proteins, and Nucleic Acids: Biotechnology Meets Materials Science. *Angew. Chem. (Int. Ed.)* **2001**, *40*, 4128–4158.

(81) Bruchez, M.; Moronne, M.; Gin, P.; Weiss, S.; Alivisatos, A. P. Semiconductor nanocrystals as fluorescent biological labels. *Science* **1998**, *281*, 2013–2016.

(82) Mattoussi, H.; Mauro, J. M.; Goldman, E. R.; Green, T. M.; Anderson, G. P.; Sundar, V. C.; Bawendi, M. G. Bioconjugation of highly luminescent colloidal CdSe−ZnS quantum dots with an engineered two-domain recombinant protein. *Physica Status Solidi B-Basic Research* **2001**, *224*, 277–283.

(83) Goldman, E. R.; Anderson, G. P.; Tran, P. T.; Mattoussi, H.; Charles, P. T.; Mauro, J. M. Conjugation of Luminescent Quantum Dots with Antibodies Using an Engineered Adaptor Protein to Provide New Reagents for Fluoroimmunoassays. *Anal. Chem.* **2002**, *74*, 841–847.

(84) Kamat, P. V.; Ebbesen, T. W.; Dimitrijevic, N. M.; Nozik, A. J. Photoelectrochemistry in semiconductor particulate systems. Part 12. Primary photochemical events in CdS semiconductor colloids as probed by picosecond laser flash photolysis, transient bleaching. *Chem. Phys. Lett.* **1989**, *157*, 384–9.

(85) Kamat, P. V.; Gopidas, K. R.; Dimitrijevic, N. M. Picosecond charge transfer processes in ultrasmall CdS and CdSe semiconductor particles. *Mol. Cryst. Liq. Cryst.* **1990**, *183*, 439–45.

(86) Kamat, P. V.; Dimitrijevic, N. M.; Nozik, A. J. Dynamic Burstein-Moss shift in semiconductor colloids. *J. Phys. Chem.* **1989**, *93*, 2873–5.

(87) Dimitrijevic, N. M.; Kamat, P. V. Transient photobleaching of small CdSe colloids in acetonitrile. Anodic decomposition. *J. Phys. Chem.* **1987**, *91*, 2096–9.

(88) Liu, C.; Bard, A. J. Effect of excess charge on band energetics (optical absorption edge and carrier redox potentials) in small semiconductor particles. *J. Phys. Chem.* **1989**, *93*, 3232–7.

(89) Ekimov, A. I.; Efros, A. L.; Shubina, T. V.; Skvortsov, A. P. Quantum-size Stark effect in semiconductor microcrystals. *J. Lumin.* **1990**, *46*, 97–100.

(90) Luangdilok, C.; Lawless, D.; Meisel, D. *Excess charge in small semiconductor particles, in Fine Particles Science and Technology*; Pelizzatti, E., Ed.; Kulwer Academic Publishers: Boston, 1996; pp 457−465.

(91) Muller, J.; Lupton, J. M.; Lagoudakis, P. G.; Schindler, F.; Koeppe, R.; Rogach, A. L.; Feldmann, J.; Talapin, D. V.; Weller, H. Wave Function Engineering in Elongated Semiconductor Nanocrystals with Heterogeneous Carrier Confinement. *Nano Lett.* **2005**, *5*, 2044–2049.

(92) Zhang, J. Z.; O'Neil, R. H.; Roberti, T. W.; McGowen, J. L.; Evans, J. E. Femtosecond studies of trapped electrons at the liquid-solid interface of aqueous CdS colloids. *Chem. Phys. Lett.* **1994**, *218*, 479–484.

(93) Norris, D. J.; Bawendi, M. G. Measurement and assignment of the size-dependent optical spectrum in CdSe quantum dots. *Phys. Rev. B* **1996**, *53*, 16338–16346.

(94) Klimov, V. I.; McBranch, D. W. Femtosecond 1P-to-1S electron relaxation in strongly confined semiconductor nanocrystals. *Phys. Rev. Lett.* **1998**, *80*, 4028–4031.

(95) Klimov, V. I.; Mikhailovsky, A. A.; McBranch, D. W.; Leatherdale, C. A.; Bawendi, M. G. Mechanisms for intraband energy relaxation in semiconductor quantum dots: The role of electron-hole interactions. *Phys. Rev. B* **2000**, *61*, R13349–R13352.

(96) Empedocles, S. A.; Neuhauser, R.; Shimizu, K.; Bawendi, M. G. Photoluminescence from single semiconductor nanostructures. *Adv. Mater.* **1999**, *11*, 1243–1256.

(97) Guyot-Sionnest, P.; Shim, M.; Matranga, C.; Hines, M. Intraband relaxation in CdSe quantum dots. *Phys. Rev. B* **1999**, *60*, R2181–R2184.

(98) Schmidt, M. E.; Blanton, S. A.; Hines, M. A.; GuyotSionnest, P. Size-dependent two-photon excitation spectroscopy of CdSe nanocrystals. *Phys. Rev. B* **1996**, *53*, 12629–12632.

(99) Krauss, T. D.; Brus, L. E. Electronic properties of single semiconductor nanocrystals: optical and electrostatic force microscopy measurements. *Mater. Sci. Eng. B* **2000**, *69*, 289–294.

(100) Klimov, V. I. Mechanisms for Photogeneration and Recombination of Multiexcitons in Semiconductor Nanocrystals: Implications for Lasing and Solar Energy Conversion. *J. Phys. Chem. B* **2006**, *110*, 16827–16845.

(101) Koberling, F.; Mews, A.; Philipp, G.; Kolb, U.; Potapova, I.; Burghard, M.; Basche, T. Fluorescence spectroscopy and transmission electron microscopy of the same isolated semiconductor nanocrystals. *Appl. Phys. Lett.* **2002**, *81*, 1116–1118.

(102) Scholes, G. D. Insights into Excitons Confined to Nanoscale Systems: Electron-Hole Interaction, Binding Energy, and Photodissociation. *ACS Nano* **2008**, *2*, 523–537.

(103) Wang, C. J.; Shim, M.; Guyot-Sionnest, P. Electrochromic nanocrystal quantum dots. *Science* **2001**, *291*, 2390–2392.

(104) Gooding, A. K.; Gomez, D. E.; Mulvaney, P. The Effects of Electron and Hole Injection on the Photoluminescence of CdSe/CdS/ZnS Nanocrystal Monolayers. *ACS Nano* **2008**, *2*, 669–676.

(105) Istrate, E.; Hoogland, S.; Sukhovatkin, V.; Levina, L.; Myrskog, S.; Smith, P. W. E.; Sargent, E. H. Carrier relaxation dynamics in lead sulfide colloidal quantum dots. *J. Phys. Chem. B* **2008**, *112*, 2757–2760.

(106) Yu, P. R.; Nedeljkovic, J. M.; Ahrenkiel, P. A.; Ellingson, R. J.; Nozik, A. J. Size dependent femtosecond electron cooling dynamics in CdSe quantum rods. *Nano Lett.* **2004**, *4*, 1089–1092.

(107) Robel, I.; Kuno, M.; Kamat, P. V. Size-Dependent electron Injection from Excited CdSe Quantum Dots into TiO_2 Nanoparticles. *J. Am. Chem. Soc.* **2007**, *129*, 4136–4137.

(108) Yu, P.; Zhu, K.; Norman, A. G.; Ferrere, S.; Frank, A. J.; Nozik, A. J. Nanocrystalline TiO_2 Solar Cells Sensitized with InAs Quantum Dots. *J. Phys. Chem. B* **2006**, *110*, 25451–25454.

(109) Marcus, R. A.; Sutin, N. Electron Transfers in Chemistry and Biology. *Biochim. Biophys. Acta* **1985**, *811*, 265.

(110) Marcus, R. A. On Theory of Electron-Transfer Reactions. 6. Unified Treatment for Homogeneous and Electrode Reactions. *J. Chem. Phys.* **1965**, *43*, 679–701.

(111) Gaal, D. A.; Hupp, J. T. Thermally activated, inverted interfacial electron transfer kinetics: High driving force reactions between tin oxide nanoparticles and electrostatically-bound molecular reactants. *J. Am. Chem. Soc.* **2000**, *122*, 10956–10963.

(112) Kuciauskas, D.; Freund, M. S.; Gray, H. B.; Winkler, J. R.; Lewis, N. S. Electron Transfer Dynamics in Nanocrystalline Titanium Dioxide Solar Cells Sensitized with Ruthenium or Osmium Polypyridyl Complexes. *J. Phys. Chem. B* **2001**, *105*, 392–403.

(113) Clifford, J. N.; Palomares, E.; Nazeeruddin, M. K.; Gratzel, M.; Nelson, J.; Li, X.; Long, N. J.; Durrant, J. R. Molecular Control of Recombination Dynamics in Dye-Sensitized Nanocrystalline TiO_2 Films: Free Energy vs Distance Dependence. *J. Am. Chem. Soc.* **2004**, *126*, 5225–5233.

(114) Huang, J.; Stockwell, D.; Huang, Z. Q.; Mohler, D. L.; Lian, T. Q. Photoinduced ultrafast electron transfer from CdSe quantum dots to Re-bipyridyl complexes. *J. Am. Chem. Soc.* **2008**, *130*, 5632–5633.

(115) Grätzel, M. Photoelectrochemical cells. *Nature* **2001**, *414*, 338.

(116) Blackburn, J. L.; Ellingson, R. J.; Micic, O. I.; Nozik, A. J. Electron relaxation in colloidal InP quantum dots with photogenerated excitons or chemically injected electrons. *J. Phys. Chem. B* **2003**, *107*, 102–109.

(117) Shen, Q.; Katayama, K.; Yamaguchi, M.; Sawada, T.; Toyoda, T. Study of ultrafast carrier dynamics of nanostructured TiO_2 films with and without CdSe quantum dot deposition using lens-free heterodyne detection transient grating technique. *Thin Solid Films* **2005**, *486*, 15–19.

(118) Hodes, G.; Howell, I. D. J.; Peter, L. M. Nanocrystalline photoelectrochemical cells. A new concept in photovoltaic cells. *J. Electrochem. Soc.* **1992**, *139*, 3136–40.

(119) Golan, Y.; Margulis, L.; Rubinstein, I.; Hodes, G. Epitaxial electrodeposition of CdSe nanocrystals on gold. *Langmuir* **1992**, *8*, 749–752.

(120) Nasr, C.; Hotchandani, S.; Kamat, P. V.; Das, S.; Thomas, K. G.; George, M. V. Electrochemical and photoelectrochemical properties of monoaza-15-Crown ether linked cyanine dyes: Photosensitization of nanocrystalline SnO_2 films. *Langmuir* **1995**, *11*, 1777–1783.

(121) Chen, S.; Murray, R. W. Electrochemical Quantized Capacitance Charging of Surface Ensembles of Gold Nanoparticles. *J. Phys. Chem. B* **1999**, *103*, 9996–10000.

(122) Chen, S.; Ingram, R. S.; Hostetler, M. J.; Pietron, J. J.; Murray, R. W.; Schaaff, T. G.; Khoury, J. T.; Alvarez, M. M.; Whetten, R. L. Gold Nanoelectrodes of Varied Size: Transition to Molecule-Like Charging. *Science* **1998**, *280*, 2098–2101.

(123) Henglein, A.; Holzwarth, A.; Mulvaney, P. Fermi level equilibration between colloidal lead and silver particles in aqueous solution. *J. Phys. Chem.* **1992**, *96*, 8700–2.

(124) Wood, A.; Giersig, M.; Mulvaney, P. Fermi Level Equilibration in Quantum Dot-Metal Nanojunctions. *J. Phys. Chem. B* **2001**, *105*, 8810–8815.

(125) Subramanian, V.; Wolf, E. E.; Kamat, P. V. Green Emission to Probe Photoinduced Charging Events in ZnO−Au Nanoparticles. Charge Distribution and Fermi-Level Equilibration. *J. Phys. Chem. B* **2003**, *107*, 7479–7485.

(126) Jakob, M.; Levanon, H.; Kamat, P. V. Charge Distribution between UV-Irradiated TiO_2 and Gold Nanoparticles. Determination of Shift in Fermi Level. *Nano Lett.* **2003**, *3*, 353–358.

(127) Subramanian, V.; Wolf, E. E.; Kamat, P. V. Catalysis with TiO_2/Au Nanocomposites. Effect of Metal Particle Size on the Fermi Level Equilibration. *J. Am. Chem. Soc.* **2004**, *126*, 4943–4950.

(128) Nenadovic, M. T.; Rajh, T.; Micic, O. I.; Nozik, A. J. Electron transfer reactions and flat-band potentials of WO_3 colloids. *J. Phys. Chem.* **1984**, *88*, 5827–30.

(129) Dimitrijevic, N. M.; Savic, D.; Micic, O. I.; Nozik, A. J. Interfacial electron-transfer equilibria and flat-band potentials of α-Fe_2O_3 and TiO_2 colloids studied by pulse radiolysis. *J. Phys. Chem.* **1984**, *88*, 4278–83.

(130) Haruta, M. Size- and support-dependency in the catalysis of gold. *Catal. Today* **1997**, *36*, 153–166.

(131) Nakanishi, T.; Ohtani, B.; Uosaki, K. Fabricaton and characterization of CdS-nanoparticle mono- and multilayers on a self-assembled monolayer of alkanedithiols on gold. *J. Phys. Chem. B* **1998**, *102*, 1571–1577.

(132) Torimoto, T.; Tsumura, N.; Nakamura, H.; Kuwabata, S.; Sakata, T.; Mori, H.; Yoneyama, H. Photoelectrochemical properties of size-quantized semiconductor photoelectrodes prepared by two-dimensional cross-linking of monodisperse CdS nanoparticles. *Electrochim. Acta* **2000**, *45*, 3269–3276.

(133) Hens, Z.; Tallapin, D. V.; Weller, H. Breaking and restoring a molecularly bridged metal/quantum dot junction. *Appl. Phys. Lett.* **2002**, *81*, 4245–4247.

(134) Ginger, D. S.; Greenham, N. C. Charge injection and transport in films of CdSe nanocrystals. *J. Appl. Phys.* **2000**, *87*, 1361–1368.

(135) Zayats, M.; Kharitonov, A. B.; Pogorelova, S. P.; Lioubashevski, O.; Katz, E.; Willner, I. Probing Photoelectrochemical Processes in Au-CdS Nanoparticle Arrays by Surface Plasmon Resonance: Application for the Detection of Acetylcholine Esterase Inhibitors. *J. Am. Chem. Soc.* **2003**, *125*, 16006–16014.

(136) Granot, E.; Patolsky, F.; Willner, I. Electrochemical assembly of a CdS semiconductor nanoparticle monolayer on surfaces: Structural properties and photoelectrochemical applications. *J. Phys. Chem. B* **2004**, *108*, 5875–5881.

(137) Granot, E.; Patolsky, F.; Willner, I. Electrochemical Assembly of a CdS Semiconductor Nanoparticle Monolayer on Surfaces: Structural Properties and Photoelectrochemical Applications. *J. Phys. Chem. B* **2004**, *108*, 5875–5881.

(138) Costi, R.; Saunders, A. E.; Elmalem, E.; Salant, A.; Banin, U. Visible light-induced charge retention and photocatalysis with hybrid CdSe-Au nanodumbbells. *Nano Lett.* **2008**, *8*, 637–641.

(139) Pons, T.; Medintz, I. L.; Sapsford, K. E.; Higashiya, S.; Grimes, A. F.; English, D. S.; Mattoussi, H. On the Quenching of Semiconductor Quantum Dot Photoluminescence by Proximal Gold Nanoparticles. *Nano Lett.* **2007**, *7*, 3157–3164.

(140) Kondon, M.; Kim, J.; Udawatte, N.; Lee, D. Origin of size-dependent energy transfer from photoexcited CdSe quantum dots to gold nanoparticles. *J. Phys. Chem. C* **2008**, *112*, 6695–6699.

(141) Kamat, P. V.; de Lind, M.; Hotchandani, S. Surface modification of CdS colloids with mercaptoethylamine. *Isr. J. Chem.* **1993**, *33*, 47–51.

(142) Shanghavi, B.; Kamat, P. V. Interparticle electron transfer in metal/semiconductor composites. Picosecond dynamics of CdS capped gold nanoclusters. *J. Phys. Chem. B* **1997**, *101*, 7675–7679.

(143) Chandrasekharan, N.; Kamat, P. V. Improving the Photoelectrochemical Performance of Nanostructured TiO_2 Films by Adsorption of Gold Nanoparticles. *J. Phys. Chem. B* **2000**, *104*, 10851–10857.

(144) Johnston, K. W.; Pattantyus-Abraham, A. G.; Clifford, J. P.; Myrskog, S. H.; MacNeil, D. D.; Levina, L.; Sargent, E. H. Schottky-quantum dot photovoltaics for efficient infrared power conversion. *Appl. Phys. Lett.* **2008**, *92*, 151115.

(145) Clifford, J. P.; Johnston, K. W.; Levina, L.; Sargent, E. H. Schottky barriers to colloidal quantum dot films. *Appl. Phys. Lett.* **2007**, *91*, 253117.

(146) Klem, E. J. D.; Shukla, H.; Hinds, S.; MacNeil, D. D.; Levina, L.; Sargent, E. H. Impact of dithiol treatment and air annealing on the conductivity, mobility, and hole density in PbS colloidal quantum dot solids. *Appl. Phys. Lett.* **2008**, *92*, Art. 212105.

(147) Koleilat, G. I.; Levina, L.; Shukla, H.; Myrskog, S. H.; Hinds, S.; Pattantyus-Abraham, A. G.; Sargent, E. H. Efficient, stable infrared

photovoltaics based on solution-cast colloidal quantum dots. *ACS Nano* **2008**, *2*, 833–840.

(148) Coffey, D. C.; Reid, O. G.; Rodovsky, D. B.; Bartholomew, G. P.; Ginger, D. S. Mapping local photocurrents in polymer/fullerene solar cells with photoconductive atomic force microscopy. *Nano Lett.* **2007**, *7*, 738–744.

(149) Gunes, S.; Neugebauer, H.; Sariciftci, N. S. Conjugated polymer-based organic solar cells. *Chem. Rev.* **2007**, *107*, 1324–1338.

(150) Tang, C. W. 2-Layer Organic Photovoltaic Cell. *Appl. Phys. Lett.* **1986**, *48*, 183–185.

(151) Shaheen, S. E.; Brabec, C. J.; Sariciftci, N. S.; Padinger, F.; Fromherz, T.; Hummelen, J. C. 2.5% efficient organic plastic solar cells. *Appl. Phys. Lett.* **2001**, *76*, 841–843.

(152) Heeger, A. J. Semiconducting and Metallic Polymers: The Fourth Generation of Polymeric Materials. *J. Phys. Chem. B* **2001**, *105*, 8475–8491.

(153) Gomez-Romero, P. Hybrid organic-inorganic materials - In search of synergic activity. *Adv. Mater.* **2001**, *13*, 163–174.

(154) Breeze, A. J.; Schlesinger, Z.; Carter, S. A.; Brock, P. J. Charge transport in TiO_2/MEH-PPV polymer photovoltaics. *Phys. Rev. B* **2001**, *6412*, n/a. art. 125205.

(155) Hoppe, H.; Sariciftci, N. S. Organic solar cells: An overview. *J. Mater. Res.* **2004**, *19*, 1924–1945.

(156) Yu, G.; Gao, J.; Hummelen, J. C.; Wudl, F.; Heeger, A. J. Polymer Photovoltaic Cells - Enhanced Efficiencies Via a Network of Internal Donor-Acceptor Heterojunctions. *Science* **1995**, *270*, 1789–1791.

(157) Campoy-Quiles, M.; Ferenczi, T.; Agostinelli, T.; Etchegoin, P. G.; Kim, Y.; Anthopoulos, T. D.; Stavrinou, P. N.; Bradley, D. D. C.; Nelson, J. Morphology evolution via self-organization and lateral and vertical diffusion in polymer: fullerene solar cell blends. *Nat. Mater.* **2008**, *7*, 158–164.

(158) Pivrikas, A.; Sariciftci, N. S.; Juska, G.; Osterbacka, R. A review of charge transport and recombination in polymer/fullerene organic solar cells. *Prog. Photovoltaics* **2007**, *15*, 677–696.

(159) Hammer, N. I.; Emrick, T.; Barnes, M. D. Quantum dots coordinated with conjugated organic ligands: new nanomaterials with novel photophysics. *Nanoscale Res. Lett.* **2007**, *2*, 282–290.

(160) Guenes, S.; Sariciftci, N. S. Hybrid solar cells. *Inorg. Chim. Acta* **2008**, *361*, 581–588.

(161) Saunders, B. R.; Turner, M. L. Nanoparticle-polymer photovoltaic cells. *Adv. Colloid Interface Sci.* **2008**, *138*, 1–23.

(162) Wei, J. H.; Coffey, D. C.; Ginger, D. S. Nucleating pattern formation in spin-coated polymer blend films with nanoscale surface templates. *J. Phys. Chem. B* **2006**, *110*, 24324–24330.

(163) Kim, Y.; Nelson, J.; Durrant, J. R.; Bradley, D. D. C.; Heo, K.; Park, J.; Kim, H.; McCulloch, I.; Heeney, M.; Ree, M.; Ha, C. S. Polymer chain/nanocrystal ordering in thin films of regioregular poly(3-hexylthiophene) and blends with a soluble fullerene. *Soft Matter* **2007**, *3*, 117–121.

(164) Coffey, D. C.; Ginger, D. S. Time-resolved electrostatic force microscopy of polymer solar cells. *Nat. Mater.* **2006**, *5*, 735–740.

(165) Gur, I.; Fromer, N. A.; Chen, C. P.; Kanaras, A. G.; Alivisatos, A. P. Hybrid Solar Cells with Prescribed Nanoscale Morphologies Based on Hyperbranched Semiconductor Nanocrystals. *Nano Lett.* **2007**, *7*, 409–414.

(166) Mattoussi, H.; Radzilowskii, L. H.; Dabbousi, B. O.; Thomas, E. L.; Bawendi, M. G.; Rubner, M. F. Electroluminescence from heterostructures of poly(phenylene vinylene) and inorganic CdSe nanocrystals. *J. Appl. Phys.* **1998**, *83*, 7965–7974.

(167) Ginger, D. S.; Greenham, N. C. Photoinduced electron transfer from conjugated polymers to CdSe nanocrystals. *Phys. Rev. B* **1999**, *59*, 10622–10629.

(168) Ginger, D. S.; Greenham, N. C. Charge separation in conjugated-polymer/nanocrystal blends. *Synth. Met.* **1999**, *101*, 425–428.

(169) Huynh, W. U.; Dittmer, J. J.; Alivisatos, A. P. Hybrid Nanorod-Polymer Solar Cells. *Science* **2002**, *295*, 2425–2427.

(170) Pientka, M.; Wisch, J.; Boger, S.; Parisi, J.; Dyakonov, V.; Rogach, A.; Talapin, D.; Weller, H. Photogeneration of charge carriers in blends of conjugated polymers and semiconducting nanoparticles. *Thin Solid Films* **2004**, *451−52*, 48–53.

(171) Pientka, M.; Dyakonov, V.; Meissner, D.; Rogach, A.; Vanderzande, D.; Weller, H.; Lutsen, L.; Vanderzande, D. Photoinduced charge transfer in composites of conjugated polymers and semiconductor nanocrystals. *Nanotechnol.* **2004**, *15*, 163–170.

(172) Liu, J.; Kadnikova, E. N.; Liu, Y.; McGehee, M. D.; Frechet, J. M. J. Polythiophene Containing Thermally Removable Solubilizing Groups Enhances the Interface and the Performance of Polymer-Titania Hybrid Solar Cells. *J. Am. Chem. Soc.* **2004**, *126*, 9486–9487.

(173) Gregg, B. A. Excitonic Solar Cells. *J. Phys. Chem. B* **2003**, *107*, 4688–4698.

(174) Sariciftci, N. S. Role of buckminsterfullerene, C_{60}, in organic photoelectric devices. *Prog. Quant. Electr.* **1995**, *19*, 131–59.

(175) Brabec, C. J.; Sariciftci, N. S.; Hummelen, J. C. Plastic Solar Cells. *Adv. Funct. Mater.* **2001**, *11*, 15–26.

(176) Salafsky, J. S. Exciton dissociation, charge transport, and recombination in ultrathin, conjugated polymer-TiO_2 nanocrystal intermixed composites. *Phys. Rev. B* **1999**, *59*, 10885–10894.

(177) Sasha, G.; Gary, H. Quantum size effects in the study of chemical solution deposition mechanisms of semiconductor films. *J. Phys. Chem.* **1994**, *98*, 5338.

(178) Yochelis, S.; Hodes, G. Nanocrystalline CdSe formation by direct reaction between Cd ions and selenosulfate solution. *Chem. Mater.* **2004**, *16*, 2740–2744.

(179) Niitsoo, O.; Sarkar, S. K.; Pejoux, C.; Ruhle, S.; Cahen, D.; Hodes, G. Chemical bath deposited CdS/CdSe-sensitized porous TiO_2 solar cells. *J. Photochem. Photobiol. A* **2006**, *181*, 306–313.

(180) Hao, E.; Yang, B.; Zhang, J.; Zhang, X.; Sun, J.; Shen, J. Assembly of alternating TiO_2/CdS nanoparticle composite films. *J. Mater. Chem.* **1999**, *8*, 1327–1328.

(181) Fang, J. J.; Wu, J. X.; Lu, X.; Shen, Y.; Lu, Z. Sensitization of nanocrystalline TiO_2 electrode with quantum sized CdSe and ZnTCPc molecules. *Chem. Phys. Lett.* **1997**, *270*, 145.

(182) Wijayantha, K. G. U.; Peter, L. M.; Otley, L. C. Fabrication of CdS quantum dot sensitized solar cells via a pressing route. *Sol. Energy Mater. Solar Cells* **2004**, *83*, 363–369.

(183) Mora-Sero, I.; Bisquert, J.; Dittrich, T.; Belaidi, A.; Susha, A. S.; Rogach, A. L. Photosensitization of TiO_2 layers with CdSe quantum dots: Correlation between light absorption and photoinjection. *J. Phys. Chem. C* **2007**, *111*, 14889–14892.

(184) Lee, J. C.; Sung, Y. M.; Kim, T. G.; Choi, H. J. TiO2-CdSe nanowire arrays showing visible-range light absorption. *Appl. Phys. Lett.* **2007**, *91*, Art. 113104.

(185) Prabakar, K.; Takahashi, T.; Nakashima, T.; Kubota, Y.; Fujishima, A. Optimization and deposition of CdS thin films as applicable to TiO_2/CdS composite catalysis. *J. Vac. Sci. Technol. A* **2006**, *24*, 1613–1617.

(186) Lopez-Luke, T.; Wolcott, A.; Xu, L. P.; Chen, S. W.; Wcn, Z. H.; Li, J. H.; De La Rosa, E.; Zhang, J. Z. Nitrogen-doped and CdSe quantum-dot-sensitized nanocrystalline TiO_2 films for solar energy conversion applications. *J. Phys. Chem. C* **2008**, *112*, 1282–1292.

(187) Si, H. Y.; Sun, Z. H.; Zhang, H. L. Photoelectrochemical response from CdSe-sensitized anodic oxidation TiO_2 nanotubes. Colloids and Surfaces. *Part A-Physicochem. Eng. Aspects* **2008**, *313*, 604–607.

(188) Shen, Q.; Yanai, M.; Katayama, K.; Sawada, T.; Toyoda, T. Optical absorption, photosensitization, and ultrafast carrier dynamic investigations of CdSe quantum dots grafted onto nanostructured SnO_2 electrode and fluorine-doped tin oxide (FTO) glass. *Chem. Phys. Lett.* **2007**, *442*, 89–96.

(189) Hotchandani, S.; Kamat, P. V. Modification of electrode surface with semiconductor colloids and its sensitization with chlorophyll a. *Chem. Phys. Lett.* **1992**, *191*, 320–6.

(190) Tena-Zaera, R.; Katty, A.; Bastide, S.; Levy-Clement, C. Annealing effects on the physical properties of electrodeposited ZnO/CdSe core-shell nanowire arrays. *Chem. Mater.* **2007**, *19*, 1626–1632.

(191) Wang, Z. L. Transmission Electron Microscopy of Shape-Controlled Nanocrystals and Their Assemblies. *J. Phys. Chem.* **2000**, *104*, 1153–1175.

(192) Gur, I.; Fromer, N. A.; Geier, M. L.; Alivisatos, A. P. Air-Stable All-Inorganic Nanocrystal Solar Cells Processed from Solution. *Science* **2005**, *310*, 462–464.

(193) Gross, D.; Susha, A. S.; Klar, T. A.; Da Como, E.; Rogach, A. L.; Feldmann, J. Charge separation in type II tunneling structures of close-packed CdTe and CdSe nanocrystals. *Nano Lett.* **2008**, *8*, 1482–1485.

(194) Lawless, D.; Kapoor, S.; Meisel, D. Bifunctional capping of CdS nano-particles and bridging to TiO_2. *J. Phys. Chem.* **1995**, *99*, 10329–10335.

(195) Baron, R.; Huang, C. H.; Bassani, D. M.; Onopriyenko, A.; Zayats, M.; Willner, I. Hydrogen-bonded CdS nanoparticle assemblies on electrodes for photoelectrochemical applications. *Angew. Chem., Int. Ed.* **2005**, *44*, 4010–4015.

(196) Kamat, P. V.; Barazzouk, S.; Hotchandani, S. Electrochemical Modulation of Fluorophore Emission at a Nanostructured Gold Film. *Angew. Chem. (Int. Ed.)* **2002**, *41*, 2764–2767.

(197) Nazeeruddin, M. K.; Kay, A.; Rodicio, I.; Humphry, B. R.; Mueller, E.; Liska, P.; Vlachopoulos, N.; Graetzel, M. Conversion of light to electricity by cis-X_2bis(2,2′-bipyridyl-4,4′-dicarboxylate)ruthenium(II) charge-transfer sensitizers (X = Cl−, Br−, I−, CN−, and SCN−) on nanocrystalline TiO_2 electrodes. *J. Am. Chem. Soc.* **1993**, *115*, 6382–90.

(198) Meyer, T. J.; et al. Molecular-Level Electron-Transfer and Excited-State Assemblies on Surfaces of Metal-Oxides and Glass. *Inorg. Chem.* **1994**, *33*, 3952–3964.

(199) Rogach, A. L.; Kornowski, A.; Gao, M.; Eychmüller, A.; Weller, H. Synthesis and Characterization of a Size Series of Extremely Small Thiol-Stabilized CdSe Nanocrystals. *J. Phys. Chem. B* **1999**, *103*, 3065–3069.

(200) Cassagneau, T.; Mallouk, T. E.; Fendler, J. H. Layer-by-layer assembly of thin film zener diodes from conducting polymers and CdSe nanoparticles. *J. Am. Chem. Soc.* **1998**, *120*, 7848–7859.

(201) Landes, C.; Burda, C.; Braun, M.; El-Sayed, M. A. Photoluminescence of CdSe nanoparticles in the presence of a hole acceptor: n-butylamine. *J. Phys. Chem. B* **2001**, *105*, 2981–2986.

(202) Landes, C. F.; Braun, M.; El-Sayed, M. A. On the nanoparticle to molecular size transition: Fluorescence quenching studies. *J. Phys. Chem. B* **2001**, *105*, 10554–10558.

(203) Sharma, S.; Pillai, Z. S.; Kamat, P. V. Photoinduced charge transfer between CdSe nanocrystals and p-phenylenediamine. *J. Phys. Chem. B* **2003**, *107*, 10088–10093.

(204) Islam, M. A.; Herman, I. P. Electrodeposition of patterned CdSe nanocrystal films using thermally charged nanocrystals. *Appl. Phys. Lett.* **2002**, *80*, 3823–3825.

(205) Islam, M. A.; Xia, Y. Q.; Steigerwald, M. L.; Yin, M.; Liu, Z.; O'Brien, S.; Levicky, R.; Herman, I. P. Addition, suppression, and inhibition in the electrophoretic deposition of nanocrystal mixture films for CdSe nanocrystals with gamma-Fe_2O_3 and Au nanocrystals. *Nano Lett.* **2003**, *3*, 1603–1606.

(206) Brown, P.; Kamat, P. V. Quantum Dot Solar Cells. Electrophoretic Deposition of CdSe−C_{60} Composite Films and Capture of Photogenerated Electrons with *n*C_{60} Cluster Shell. *J. Am. Chem. Soc.* **2008**, *130*, 8890–8891.

(207) Rosenwaks, Y.; Thacker, B. R.; Nozik, A. J.; Ellingson, R. J.; Burr, K. C.; Tang, C. L. Ultrafast photoinduced electron transfer across semiconductor-liquid interfaces in the presence of electric fields. *J. Phys. Chem.* **1994**, *98*, 2739–2741.

(208) Shen, Q.; Arae, D.; Toyoda, T. Photosensitization of nanostructured TiO_2 with CdSe quantum dots: effects of microstructure and electron transport in TiO_2 substrates. *J. Photochem. Photobiol. A* **2004**, *164*, 75–80.

(209) Leschkies, K. S.; Divakar, R.; Basu, J.; Enache-Pommer, E.; Boercker, J. E.; Carter, C. B.; Kortshagen, U. R.; Norris, D. J.; Aydil, E. S. Photosensitization of ZnO nanowires with CdSe quantum dots for photovoltaic devices. *Nano Lett.* **2007**, *7*, 1793–1798.

(210) Diguna, L. J.; Shen, Q.; Kobayashi, J.; Toyoda, T. High efficiency of CdSe quantum-dot-sensitized TiO_2 inverse opal solar cells. *Appl. Phys. Lett.* **2007**, *91*, n/a.

(211) Shen, Q.; Kobayashi, J.; Diguna, L. J.; Toyoda, T. Effect of ZnS coating on the photovoltaic properties of CdSe quantum dot-sensitized solar cells. *J. Appl. Phys.* **2008**, *103*, n/a.

(212) Lee, J. C.; Kim, T. G.; Choi, H. J.; Sung, Y. M. Enhanced photochemical response of TiO_2/CdSe heterostructured nanowires (vol 7, pg 2591, 2007). *Cryst. Growth Des.* **2008**, *8*, 750–750.

(213) Shen, Q.; Katayama, K.; Sawada, T.; Yamaguchi, M.; Toyoda, T. Optical Absorption, Photoelectrochemical, and Ultrafast Carrier Dynamic Investigations of TiO_2 Electrodes Composed of Nanotubes and Nanowires Sensitized with CdSe Quantum Dots. *Jpn. J. Appl. Phys.* **2006**, *45*, 5569–5574.

(214) Chong, S. V.; Suresh, N.; Xia, J.; Al-Salim, N.; Idriss, H. TiO_2 nanobelts/CdSSe quantum dots nanocomposite. *J. Phys. Chem. C* **2007**, *111*, 10389–10393.

(215) Kamat, P. V.; Haria, M.; Hotchandani, S. C_{60} Cluster as an Electron Shuttle in a Ru(II)-Polypyridyl Sensitizer Based Photochemical Solar Cell. *J. Phys. Chem. B* **2004**, *108*, 5166–5170.

(216) Kamat, P. V.; Barazzouk, S.; Hotchandani, S.; Thomas, K. G. Nanostructured Thin Films of C_{60}−Anline Dyad Clusters. Electrodeposition, Charge Separation and Photoelectrochemistry. *Chem., Eur. J.* **2000**, *6*, 3914–3921.

(217) Hasobe, T.; Kashiwagi, Y.; Absalom, M. A.; Sly, J.; Hosomizu, K.; Crossley, M. J.; Imahori, H.; Kamat, P. V.; Fukuzumi, S. *Supramolecular Photovoltaic Cells Composed of Clusterized Fullerenes with Porphyrin Dendrimers and Porphyrin-Alkanethiolate Protected-Gold Nanoparticles*; Annual meeting of the Electrochemical Society; The Electrochemical Society: San Antonio, TX, 2004.

(218) Hasobe, T.; Saito, K.; Kamat, P. V.; Troiani, V.; Qiu, H.; Solladié, N.; Kim, K. S.; Park, J. K.; Kim, D.; D'Souza, F.; Fukuzumi, S. Organic Solar Cells. Supramolecular Composites of Porphyrins and Fullerenes Organized by Polypeptide Structures as Light Harvesters. *J. Mater. Chem.* **2007**, *17*, 4160–4170.

(219) Yu, G.; Heeger, A. J. Charge separation and photovoltaic conversion in polymer composites with internal donor/acceptor heterojunctions. *J. Appl. Phys.* **1995**, *78*, 4510–4515.

(220) Sariciftci, N. S.; Heeger, A. J. Photophysics of semiconducting polymer−C_{60} composites: A comparative study. *Synth. Met.* **1995**, *70*, 1349–52.

(221) Tada, K.; Onoda, M. Loading Fullerene into a Conjugated Polymer Without Chemical Modification. *Adv. Funct. Mater.* **2004**, *1*, 139–144.

(222) Hasobe, T.; Imahori, H.; Kamat, P. V.; Fukuzumi, S. Photovoltaic Cells using Composite Nanoclusters of Porphyrins and Fullerenes with Gold Nanoparticles. *J. Am. Chem. Soc.* **2005**, *127*, 1216–1228.

(223) Biebersdorf, A.; Dietmuller, R.; Susha, A. S.; Rogach, A. L.; Poznyak, S. K.; Talapin, D. V.; Weller, H.; Klar, T. A.; Feldmann, J. Semiconductor Nanocrystals Photosensitize C_{60} Crystals. *Nano Lett.* **2006**, *6*, 1559–1563.

(224) Boulesbaa, A.; Issac, A.; Stockwell, D.; Huang, Z.; Huang, J.; Guo, J.; Lian, T. Ultrafast Charge Separation at CdS Quantum Dot/Rhodamine B Molecule Interface. *J. Am. Chem. Soc.* **2007**, *129*, 15132–15133.

(225) Thomas, K. G.; Biju, V.; George, M. V.; Guldi, D. M.; Kamat, P. V. Photoinduced Charge Separation and Stabilization in Clusters of a Fullerene−Aniline Dyad. *J. Phys. Chem. B* **1999**, *103*, 8864–8869.

(226) Barazzouk, S.; Hotchandani, S.; Kamat, P. V. Unusual Electrocatalytic Behavior of Ferrocene Bound Fullerene Cluster Films. *J. Mater. Chem.* **2002**, *12*, 2021–2025.

(227) Sykora, M.; Petruska, M. A.; Alstrum-Acevedo, J.; Bezel, I.; Meyer, T. J.; Klimov, V. I. Photoinduced Charge Transfer between CdSe Nanocrystal Quantum Dots and Ru-Polypyridine Complexes. *J. Am. Chem. Soc.* **2006**, *128*, 9984–9985.

(228) Hammel, E.; Tang, X.; Trampert, M.; Schmitt, T.; Mauthner, K.; Eder, A.; Potschke, P. Carbon nanofibers for composite applications. *Carbon* **2004**, *42*, 1153–1158.

(229) Wang, J.; Deo, R. P.; Poulin, P.; Mangey, M. Carbon nanotube fiber microelectrodes. *J. Am. Chem. Soc.* **2003**, *125*, 14706–14707.

(230) Rajesh, B.; Thampi, K. R.; Bonard, J. M.; Mathieu, H. J.; Xanthopoulos, N.; Viswanathan, B. Conducting polymeric nanotubules as high performance methanol oxidation catalyst support. *Chemical Communications* **2003**, 2022–2023.

(231) Kamat, P. V. Carbon Nanomaterials: Building Blocks in Energy Conversion Devices. *Interface* **2006**, *15*, 45–47.

(232) Kamat, P. V. Harvesting photons with carbon nanotubes. *Nanotoday* **2006**, *1*, 20–27.

(233) Baughman, R. H.; Zakhidov, A. A.; de Heer, W. A. Carbon nanotubes - the route toward applications. *Science* **2002**, *297*, 787–792.

(234) Sheeney-Haj-Khia, L.; Basnar, B.; Willner, I. Efficient generation of photocurrents by using CdS/Carbon nanotube assemblies on electrodes. *Angew. Chem., Int. Ed.* **2005**, *44*, 78–83.

(235) Huang, Q.; Gao, L. Synthesis and characterization of CdS/multiwalled carbon nanotube heterojunctions. *Nanotechnol.* **2004**, *15*, 1855–1860.

(236) Banerjee, S.; Wong, S. S. In situ quantum dot growth on multiwalled carbon nanotubes. *J. Am. Chem. Soc.* **2003**, *125*, 10342–10350.

(237) Banerjee, S.; Wong, S. S. Formation of CdSe nanocrystals onto oxidized, ozonized single-walled carbon nanotube surfaces. *Chemical Communications* **2004**, 1866–1867.

(238) Chaudhary, S.; Kim, J. H.; Singh, K. V.; Ozkan, M. Fluorescence microscopy visualization of single-walled carbon nanotubes using semiconductor nanocrystals. *Nano Lett.* **2004**, *4*, 2415–2419.

(239) Haremza, J. M.; Hahn, M. A.; Krauss, T. D. Attachment of single CdSe nanocrystals to individual single-walled carbon nanotubes. *Nano Lett.* **2002**, *2*, 1253–1258.

(240) Ravindran, S.; Chaudhary, S.; Colburn, B.; Ozkan, M.; Ozkan, C. S. Covalent coupling of quantum dots to multiwalled carbon nanotubes for electronic device applications. *Nano Lett.* **2003**, *3*, 447–453.

(241) Shan, Y.; Gao, L. In situ coating carbon nanotubes with wurtzite ZnS nanocrystals. *J. Am. Ceram. Soc.* **2006**, *89*, 759–762.

(242) Banerjee, S.; Wong, S. S. Synthesis and characterization of carbon nanotube-nanocrystal heterostructures. *Nano Lett.* **2002**, *2*, 195–200.

(243) Kalbac, M.; Frank, O.; Kavan, L.; Zukalova, M.; Prochazka, J.; Klementova, M.; Dunsch, L. Heterostructures from single-wall carbon nanotubes and TiO_2 nanocrystals. *J. Electrochem. Soc.* **2007**, *154*, K19–K24.

(244) Han, W. Q.; Zettl, A. Coating single-walled carbon nanotubes with tin oxide. *Nano Lett.* **2003**, *3*, 681–683.

(245) Vietmeyer, F.; Seger, B.; Kamat, P. V. Anchoring ZnO Particles on Functionalized Single Wall Carbon Nanotubes. Excited State Interactions and Charge Collection. *Adv. Mater.* **2007**, *19*, 2935–2940.

(246) Juarez, B. H.; Klinke, C.; Kornowski, A.; Weller, H. Quantum Dot Attachment and Morphology Control by Carbon Nanotubes. *Nano Lett.* **2007**, *7*, 3564–3568.

(247) Shi, J.; Qin, Y.; Wu, W.; Li, X.; Guo, Z.-X.; Zhu, D. In situ synthesis of CdS nanoparticles on multi-walled carbon nanotubes. *Carbon* **2004**, *42*, 455–458.

(248) Robel, I.; Bunker, B.; Kamat, P. V. SWCNT-CdS nanocomposite as light harvesting assembly. Photoinduced charge transfer interactions. *Adv. Mater.* **2005**, *17*, 2458–2463.

(249) Lee, W.; Lee, J.; Lee, S.; Yi, W.; Han, S. H.; Cho, B. W. Enhanced charge collection and reduced recombination of CdS/TiO_2 quantum-dots sensitized solar cells in the presence of single-walled carbon nanotubes. *Appl. Phys. Lett.* **2008**, *92*, Art. 153510.

(250) Hu, L.; Zhao, Y. L.; Ryu, K.; Zhou, C.; Stoddart, J. F.; Gruner, G. Light-induced charge transfer in Pyrene/CdSe-SWNT hybrids. *Adv. Mater.* **2008**, *20*, 939–946.

(251) Kongkanand, A.; Domínguez, R. M.; Kamat, P. V. Single Wall Carbon Nanotube Scaffolds for Photoelectrochemical Solar Cells. Capture and Transport of Photogenerated Electrons. *Nano Lett.* **2007**, *7*, 676–680.

(252) Jung, K. H.; Hong, J. S.; Vittal, R.; Kim, K. J. Enhanced photocurrent of dye-sensitized solar cells by modification of TiO_2 with carbon nanotubes. *Chem. Lett.* **2002**, 864–865.

(253) Kongkanand, A.; Kamat, P. V. Electron Storage in Single Wall Carbon Nanotubes. Fermi Level Equilibration in Semiconductor−SWCNT Suspensions. *ACS Nano* **2007**, *1*, 13–21.

(254) Yu, H.; Quan, X.; Chen, S.; Zhao, H. TiO_2-Multiwalled Carbon Nanotube Heterojunction Arrays and Their Charge Separation Capability. *J. Phys. Chem. C* **2007**, *111*, 12987–12991.

(255) Brown, P. R.; Takechi, K.; Kamat, P. V. Single-Walled Carbon Nanotube Scaffolds for Dye-Sensitized Solar Cells. *J. Phys. Chem. C* **2008**, *112*, 4776–4782.

(256) Williams, G.; Seger, B.; Kamat, P. V. TiO_2-Graphene Nanocomposites. UV-Assisted Photocatalytic Reduction of Graphene Oxide. *ACS Nano* **2008**, *2*, 1487–1491.

(257) Muszynski, R.; Seger, B.; Kamat, P. Decorating Graphene Sheets with Gold Nanoparticles. *J. Phys. Chem. C* **2008**, *112*, 5263–5266.

(258) Mor, G. K.; Varghese, O. K.; Paulose, M.; Shankar, K.; Grimes, C. A. A review on highly ordered, vertically oriented TiO_2 nanotube arrays: Fabrication, material properties, and solar energy applications. *Sol. Energy Mater. Solar Cells* **2006**, *90*, 2011–2075.

(259) Kuno, M. An overview of solution-based semiconductor nanowires: synthesis and optical studies. *Phys. Chem. Chem. Phys.* **2008**, *10*, 620–639.

(260) Kar, S.; Santra, S. ZnO Nanotube Arrays and Nanotube-Based Paint-Brush Structures: A Simple Methodology of Fabricating Hierarchical Nanostructures with Self-Assembled Junctions and Branches. *J. Phys. Chem. C* **2008**, *112*, 8144–8146.

(261) Hsu, M. C.; Leu, I. C.; Sun, Y. M.; Hon, M. H. Fabrication of CdS@TiO_2 coaxial composite nanocables arrays by liquid-phase deposition. *J. Cryst. Growth* **2005**, *285*, 642–648.

(262) Yin, Y. X.; Jin, Z. G.; Hou, F. Enhanced solar water-splitting efficiency using core/sheath heterostructure CdS/TiO_2 nanotube arrays. *Nanotechnology* **2007**, 18.

(263) Maiolo, J. R.; Atwater, H. A.; Lewis, N. S. Macroporous silicon as a model for silicon wire array solar cells. *J. Phys. Chem. C* **2008**, *112*, 6194–6201.

(264) Spurgeon, J. M.; Atwater, H. A.; Lewis, N. S. A comparison between the behavior of nanorod array and planar Cd(Se, Te) photoelectrodes. *J. Phys. Chem. C* **2008**, *112*, 6186–6193.

(265) Hu, L.; Chen, G. Analysis of Optical Absorption in Silicon Nanowire Arrays for Photovoltaic Applications. *Nano Lett.* **2007**, *7*, 3249–3252.

(266) Maiolo, J. R.; Kayes, B. M.; Filler, M. A.; Putnam, M. C.; Kelzenberg, M. D.; Atwater, H. A.; Lewis, N. S. High aspect ratio silicon wire array photoelectrochemical cells. *J. Am. Chem. Soc.* **2007**, *129*, 12346.

(267) Kayes, B. M.; Filler, M. A.; Putnam, M. C.; Kelzenberg, M. D.; Lewis, N. S.; Atwater, H. A. Growth of vertically aligned Si wire arrays over large areas (> 1 cm^2) with Au and Cu catalysts. *Appl. Phys. Lett.* **2007**, *91*, n/a Art. 103110.

(268) Gu, Y.; Romankiewicz, J. P.; David, J. K.; Lensch, J. L.; Lauhon, L. J. Quantitative measurement of the electron and hole mobility-lifetime products in semiconductor nanowires. *Nano Lett.* **2006**, *6*, 948–952.

(269) Peng, K. Q.; Wang, X.; Lee, S. T. Silicon nanowire array photoelectrochemical solar cells. *Appl. Phys. Lett.* **2008**, *92*, 3.

(270) Goodey, A. P.; Eichfeld, S. M.; Lew, K. K.; Redwing, J. M.; Mallouk, T. E. Silicon Nanowire Array Photolectrochemical Cells. *J. Am. Chem. Soc.* **2007**, *129*, 12344–12345.

(271) Kelzenberg, M. D.; Turner-Evans, D. B.; Kayes, B. M.; Filler, M. A.; Putnam, M. C.; Lewis, N. S.; Atwater, H. A. Photovoltaic measurements in single-nanowire silicon solar cells. *Nano Lett.* **2008**, *8*, 710–714.

(272) Robel, I.; Kamat, P. V.; Kuno, M. K. Exciton Recombination in CdSe nanowires. Bimolecular to three-particle Auger Kinetics. *Nano Lett.* **2006**, *6*, 1344–1349.

(273) Protasenko, V.; Gordeyev, S.; Kuno, M. Spatial and intensity modulation of nanowire emission induced by mobile charges. *J. Am. Chem. Soc.* **2007**, *129*, 13160–13171.

(274) Protasenko, V. V.; Hull, K. L.; Kuno, M. Disorder-Induced Optical Heterogeneity in Single CdSe Nanowires. *Adv. Mater.* **2005**, *17*, 2942–2949.

(275) Yu, Y. H.; Protasenko, V.; Jena, D.; Xing, H. L.; Kuno, M. Photocurrent polarization anisotropy of randomly oriented nanowire networks. *Nano Lett.* **2008**, *8*, 1352–1357.

(276) Glennon, J. J.; Buhro, W. E.; Loomis, R. A. Simple surface-trap-filling model for photoluminescence blinking spanning entire CdSe quantum wires. *J. Phys. Chem. C* **2008**, *112*, 4813–4817.

(277) Yang, C. C.; Li, S. Size, dimensionality, and constituent stoichiometry dependence of bandgap energies in semiconductor quantum dots and wires. *J. Phys. Chem. C* **2008**, *112*, 2851–2856.

(278) Rakovich, Y. P.; Volkov, Y.; Sapra, S.; Susha, A. S.; Doblinger, M.; Donegan, J. F.; Rogach, A. L. CdTe nanowire networks: Fast self-assembly in solution, internal structure, and optical properties. *J. Phys. Chem. C* **2007**, *111*, 18927–18931.

(279) Glennon, J. J.; Tang, R.; Buhro, W. E.; Loomis, R. A. Synchronous Photoluminescence Intermittency (Blinking) along Whole Semiconductor Quantum Wires. *Nano Lett.* **2007**, *7*, 3290–3295.

(280) Wang, F.; Yu, H.; Li, J.; Hang, Q.; Zemlyanov, D.; Gibbons, P. C.; Wang, L. W.; Janes, D. B.; Buhro, W. E. Spectroscopic properties of colloidal indium phosphide quantum wires. *J. Am. Chem. Soc.* **2007**, *129*, 14327–14335.

JP806791S